Spatial organization of *Clostridium difficile* S-layer biogenesis

Peter Oatley[1†], Joseph A. Kirk[1], Simon Jones[2], Robert P. Fagan[1]

[1] The Florey Institute, Department of Molecular Biology and Biotechnology, University of Sheffield, S10 2TN, UK

[2] Department of Chemistry, University of Sheffield, S3 7HF, UK

† Corresponding author: p.oatley@sheffield.ac.uk

Abstract

Surface layers (S-layers) are protective protein coats which form around all archaea and most bacterial cells. *Clostridium difficile* is a gram-positive bacterium with an S-layer covering its peptidoglycan cell wall. The S-layer in *C. difficile* is constructed mainly of S-layer protein A (SlpA), which is a key virulence factor for these bacteria and an absolute requirement for disease. Studying the formation and maintenance of the *C. difficile* S-layer will allow the discovery of specific therapeutic interventions in the future. Here we use microscopy to examine the subcellular localization of S-layer growth and SlpA secretion. We observed formation of S-layer at specific sites that coincide with cell wall synthesis, while conversely the secretion of SlpA from the cell is delocalized. We conclude that this delocalized secretion of SlpA leads to a pool of precursor in the cell wall which is available to repair openings in the S-layer formed during cell growth or following damage.

Introduction

Clostridium difficile infection (CDI) of the gut is the major cause of antibiotic associated diarrhoea (Hull & Beck, 2004) and can lead severe inflammatory complications (Napolitano & Edmiston, 2017). This gram-positive bacterium has its cell wall encapsulated with a surface-layer (S-layer). The S-layer is a proteinaceous, paracrystalline array which acts as a protective semipermeable shell which can interact with the host (Merrigan et al., 2013) and is essential for virulence (Kirk et al., 2017). In *C. difficile* the S-layer consists mainly of SlpA, the most abundant surface protein (Wright et al., 2005). SlpA is produced as a pre-protein (Figure 1A) that is secreted and processed by Cwp84 into low molecular weight (LMW) and high molecular weight (HMW) SLP subunits (Kirby et al., 2009),(Figure 1B). These two subunits form a heterodimeric complex which can then be incorporated into the crystalline lattice of the S-layer, that is anchored to cell wall polysaccharide PS-II via three cell wall binding (CWB2) motifs within the HMW region (Willing et al., 2015) (Figure 1A).

The production and secretion of S-layer components are energetically expensive for the cell, suggesting that the process will display evolved efficiency. However, it is not yet clear how S-layer formation is spatially regulated and whether SlpA is targeted to areas of cellular growth before or after secretion (Figure 1C). *C. difficile* express two homologs of the *E. coli* cytosolic protein export ATPase, SecA: SecA1 and SecA2 (Fagan & Fairweather, 2011). These two SecAs are thought to promote post-translational secretion through the general secretory (Sec) pathway. SecA2 is required for efficient SlpA secretion (Fagan & Fairweather, 2011) and is encoded adjacent to *slpA* on the chromosome (Monot et al., 2011). It has been shown that some SecA2 systems secret specific substrates (reviewed by (Bensing, Seepersaud, Yen, & Sullam, 2014)) which may ease the burden on the general Sec system and help to spatially or temporally regulate secretion.

As an obligate anaerobe (Ransom, Ellermeier, & Weiss, 2015), *C. difficile* has been notoriously difficult to visualize using standard microscopy techniques with commonly used oxygen-dependent fluorescent proteins and this is further complicated by intrinsic autofluorescence in the green spectrum. To circumvent these problems, we have used a variety of labeling techniques to avoid the requirement for oxygen maturation and any overlap with autofluorescence. Using fluorescence microscopy, we identified areas of S-layer biogenesis and SlpA secretion to determine if this S-layer component is specifically targeted to growing parts of the cell. Firstly, we probed the localization of newly synthesized S-layer which was

detected at discrete regions which coincided with areas of new cell wall biosynthesis. We continued by studying the internal localization of SecA2 and SlpA, discovering that SlpA is secreted all over the cytoplasmic membrane. Having observed delocalized secretion of SlpA yet localized new surface S-layer we conclude that there is a pool of SlpA that resides within the cell wall which is available to seep out and construct regions of the developing S-layer.

Results

Newly synthesized S-layer co-localizes with areas of new cell wall

During exponential growth, *C. difficile* cells are constantly growing and dividing, requiring the production of new peptidoglycan cell wall and the accompanying S-layer. Peptidoglycan can be labelled by growing *C. difficile* cells in the presence of the fluorescent D-amino acid, HCC-amino-D-alanine (HADA), (Kuru et al., 2012). Chasing cell wall staining with unlabeled media reveals sites of newly synthesized peptidoglycan that appear less intense for HADA at dividing septum (Figure 2S1). Combining this with the inducible expression of the immunologically distinct $SlpA_{R20291}$ in *C. difficile* strain 630 (Figure 2S2A), allowed areas of newly assembled S-layer to be visualized by immunofluorescence (Figure 2A and 2S2B). Tracing the intensity of cell wall staining with the signal from newly synthesized surface SlpA reveals a crude anti-correlation (Figure 2B and 2S3) and suggests that new S-layer is formed at areas of newly formed underlying cell wall. The areas of newly synthesized cell wall that are void of $SlpA_{R20291}$ signal are likely to be filled with endogenous $SlpA_{630}$ that is expressed at much higher levels, observed in extracellular extracts (Figure 2S2A).

During cell division, at the septum, a large amount of new surface SlpA can be detected (Figure 3). This staining pattern suggests that S-layer is actively being formed on the mother cell over the newly synthesized cell wall, preparing each daughter cell with a new S-layer cap before cell division is complete. Numerous cells display areas of new cell wall at one of their poles that co-insides with new S-layer staining (Figure 3), we interpret these as new daughter cells that have completed cell division during the HADA stain chase. New polar S-layer can be sorted into three categories: staining distributed over the whole cell cap, on the tip of the cap or at the sides of the new cap close to the older cell wall (Figure 3). Daughter cells with their poles completely covered in new S-layer have most likely expressed $SlpA_{R20291}$ throughout cell division and have $SlpA_{R20291}$ distributed all over the new S-layer cap. The apex of the cell cap

marks the final place of new daughter cell formation and those caps stained just at the tip have probably expressed $SlpA_{R20291}$ towards the final stages of division as the two daughter cells separate and the cap is completed. Areas stained at the connecting edge between the pole and the main body of the cell must represent areas of growth once the S-layer cap was fully formed when cell division was completed. Together, these staining patterns support the hypothesis that S-layer is assembled on the mother cell at the septum to form polar caps for the daughter cells to maintain a continuous protective barrier following cell separation.

SecA2 localization in C. difficile

As newly synthesized S-layer is formed at specific points on the cell surface (Figure 3) we wanted to identify if these areas correlate with concentrated points of SlpA secretion from the cytosol. Having designated sites of secretion would allow the efficient targeting of S-layer precursors to where they are needed. As it has been shown that SecA2 is essential for cell survival (Dembek et al., 2015) and performs a critical role in SlpA secretion (Fagan & Fairweather, 2011), we assumed that intracellular positioning of SecA2 will reveal where SlpA is secreted. To confirm this, we set out to create a functional, fluorescently tagged SecA2 for monitoring SecA2 localization by microscopy. A *C. difficile* strain 630 mutant was generated that encodes a C-terminal SNAP-tagged SecA2 (SecA2-SNAP) on the genome in the original locus and under the control of the native promoter. SecA2-SNAP was the only SecA2 protein detected in membrane fractions by western immunoblot analysis (Figure 4S1A) and, when stained with TMR-Star, this protein species was the only one visualized by in-gel fluorescence (Figure 4S1B). Cells expressing SecA2-SNAP displayed similar growth dynamics to the wild-type parental strain (Figure 4S1C), suggesting that the fusion protein is fully functional as SecA2 is essential for growth. Imaging cells by widefield microscopy revealed that SecA2 is distributed throughout the cell and not localized to specific areas (Figure 4A). Higher resolution, Airyscan confocal images displayed the same widespread distribution but with pockets of higher intensity signal (Figure 4B). By combining SecA2 localization with HADA chase staining and new S-layer labelling, no correlation between SecA2 within the cell and areas of newly synthesized S-layer on the cell periphery could be determined (Figure 4B). Together these data suggest that SecA2 is not the determining factor in localization of new S-layer growth.

SlpA secretion from C. difficile

Although SecA2 was visualized throughout the cell, SecA2 has additional secretory substrates so it is possible that secretion of SlpA itself may be localized. Although immunofluorescence has been used to detect surface SlpA, S-layer pore size is thought to be too small to allow access of antibodies to protein located in the cell wall or indeed within the cell (Fagan & Fairweather, 2014). To discover where SlpA is being secreted from the cell, two different SlpA fusion proteins were constructed, an SlpA-SNAP fusion that can be secreted and is found in the extracellular fraction and a SNAP tagged SlpA-dihydrofolate reductase (SlpA-DHFR) fusion that associates with the membrane cell fraction (Figure 5A & 5S1A). DHFR is a fast folding protein that has been used to block and probe protein translocation mechanisms for many years (Arkowitz, Joly, & Wickner, 1993; Bonardi et al., 2011; Eilers & Schatz, 1986; Rassow et al., 1989). Expressing SlpA-DHFR decreases the secretion of native *C. difficile* extracellular proteins (Figure 5S1B) and leads to the build-up of precursor SlpA within the cell (Figure 5S2A). The decrease in extracellular proteins is also dependent on the SlpA-DHFR signal sequence (Figure 5S1B). Together these findings show that SlpA-DHFR fusion used in this investigation is specifically targeted to and occupies the same secretory channel required for wild-type SlpA secretion. To prevent protein secretion, the DHFR domain must first fold correctly (Arkowitz et al., 1993) and will therefore only prevent secretion via the post-translational pathway. The lack of SlpA-DHFR signal in the extracellular fraction (Figure 5S1A) shows for the first time that SlpA is exclusively post-translationally translocated. Using these two SNAP fusion proteins we can now probe the intercellular localization of SlpA secretion (SlpA-DHFR-SNAP) and localization once secreted (SlpA-SNAP).

Widefield images display a diffuse SlpA-SNAP signal on the cell surface with a halo of TMR-Star signal surrounding most of the cells (Figure 5B and C). Surface intensity plots reveal a broad cross-section of TMR-Star intensity across the cell width (Phase vs TMR-Star signal, Figure 5D). Within these cross-sections there are flat peaks of TMR-Star signal with smaller peaks towards the cell periphery (Figure 5D), this correlates with the large in-gel florescence signal observed for SlpA-SNAP-TMR-Star in the extracellular fraction of cells (Figure 5S1A). Cells expressing SlpA-DHFR-SNAP show some heterogeneity of expression (Figure 5E and F), perhaps caused by leaky expression leading to a negative selective pressure for the plasmid and the drastic effects this DHFR fusion protein has on secretion (Figure 5S1C). Again, the signal from SlpA-DHFR-SNAP appears diffuse throughout the cell and not located at specific sites (Figure 5E and F). Signal intensity traces reveal a narrow TMR-Star signal peak towards the interior of the cell (Figure 5G), suggesting a more intracellular location for SlpA-DHFR-

SNAP than SlpA-SNAP which fits with SlpA-DHFR-SNAP being trapped in the cell at the membrane (Figure 5S1A). The distribution of signal in these images suggest that SlpA secretion occurs all over the cell and not just at sites where new S-layer is being formed.

Discussion

For an S-layer to function correctly it must completely encapsulate the cell (de la Riva, Willing, Tate, & Fairweather, 2011; Kirk et al., 2017). We propose here that S-layer is assembled at areas of newly synthesized peptidoglycan to maintain a stable S-layer that continually protects the *C. difficile* cell. Although newly synthesized SlpA is secreted from all regions of the cell, only a relatively small proportion of this was detected at the surface. This irregularity suggests that *C. difficile* possess reserves of SlpA beneath the S-layer in the cell wall (Figure 6). Although excess SlpA production and storage will be quite energetically expensive for the cell, this reservoir of SlpA could provide a positive fitness advantage by allowing cells to respond quickly to repair gaps in this important barrier (Figure 6). Examples of self-repair mechanisms are present thorough all forms of life from intracellular vesicular mediated membrane healing (McNeil & Baker, 2001; Tang & Marshall, 2017) up to a tissue level such as wound healing (Greaves, Ashcroft, Baguneid, & Bayat, 2013). In addition to allowing rapid repair, having a stockpile of SlpA in the cell wall, *C. difficile* may also create a buffer so less *de novo* SlpA translation and translocation is required to safely complete cell division. The amount of SlpA that lays below the S-layer should be studied further to determine what proportion of extracellular SlpA is part of the S-layer and how much is in reserve.

Although the S-layer is a rigid structure (Mescher & Strominger, 1976), fractures in the S-layer must form to allow the cells to grow. Our data suggests that new SlpA emerges through these gaps to be incorporated into the crystalline lattice. Higher resolution imaging techniques may allow direct observation these gaps in the S-layer and how the separate S-layer sections assemble. Future work could also examine the localization of intracellular cytoskeletal and motor proteins that power cell growth (Colavin, Shi, & Huang, 2018) and how the localization of these relate to areas of newly forming cell wall and S-layer along the lateral wall.

We have also demonstrated for the first time that SlpA is secreted post-translationally. Proteins transported in this way usually interact with cytosolic chaperones that prevent folding prior to translocation (Kim & Kendall, 2000). The identity of these chaperones and the exact role

SecA2 plays in SlpA secretion has yet to be determined. Since SlpA must undergo a post-secretion protease modification (Figure 1) (Kirby et al., 2009), having a dwell time in the cell wall will allow time for correct processing. However this also poses the question of how S-layer components located there are prevented from oligomerizing (Takumi, Koga, Oka, & Endo, 1991) prior to assembly at the surface. It is tempting to speculate that the S-layer assembly pathway may also involve extracellular chaperones to facilitate processing and targeting while preventing premature self-assembly. The revelation that there is a pool of SlpA in the cell wall and the accessibility of the cell wall to drugs may provide opportunities for the identification of novel narrow spectrum targets that affect the assembly of this essential virulence factor.

In summary, we have found that S-layer is formed at sites of cell wall synthesis and there is an underlying supply of the S-layer precursor, SlpA, located throughout the cell wall.

.

Methods

Media and Growth Conditions

All strains, plasmids and oligonucleotides used in this investigation are displayed in Table 1. CA434 and NEB5α *E. coli* were grown in LB broth or on LB agar supplemented with 15 µg/ml chloramphenicol for plasmid selection. *C. difficile* were grown in reduced TY (3% Bacto tryptose, 2% yeast extract) broth or on Brain Heart Infusion agar under strict anaerobic conditions. Cultures were supplemented with 15 µg/ml thiamphenicol when selecting for plasmids.

For SlpA-DHFR-Strep expression, bacteria were subcultured from overnight cultures to an OD_{600} of 0.05, grown for 30 minutes then supplemented with 200 µM methotrexate. Bacteria were then grown for a further 30 minutes before expression of SlpA-DHFR-Strep was induced with 20 ng/ml anhydrotetracycline (Atc). Bacteria were grown for a further 3 hours before harvesting at 4,000 xg, for 10 min at 4°C.

Molecular Biology

Chemically competent *E. coli* were transformed by heat shock using standard methods and plasmids were transferred to *C. difficile* strain 630 by conjugation using the *E. coli* donor strain CA434 (Kirk & Fagan, 2016). Standard molecular biology techniques were used for restriction digest and ligations. DNA modifications were performed using Phusion High-Fidelity DNA Polymerase (Thermo Fisher) and Q5 Site-Directed Mutagenesis Kit (NEB) as per manufacturers' instructions.

Gene editing of *C. difficile* 630 was achieved through allele exchange using a construct based on pMTLsc7315 as described by Cartman *et al* (Cartman, Kelly, Heeg, Heap, & Minton, 2012).

Microscopy

TMR-Star Staining: cells were grown from an OD 0.05 to 0.4 and treated with 250 µM TMR-Star for at least 30 minutes. Transient expression of SlpA-SNAP or SlpA-DHFR-SNAP was induced for 10 minutes with 10 ng/ml Atc or 20 ng/ml for 1 hour for in-gel fluorescence experiments.

HADA Staining: Cells were grown to an OD_{600} of approximately 0.1 before the addition of 0.5 mM HADA and continued growth for at least 2 hours to an OD_{600} of 0.5-0.6. To chase the

HADA staining, cells were subsequently harvested at 4,000 x g for 5 minutes, with care being taken not to expose the cells to air, washed once by resuspension in 8 ml reduced TY and finally resuspended in 2x the original volume of reduced TY media. The cells were then grown for 25 minutes before inducing the expression of $SlpA_{R20291}$ with 100 ng/ml Atc for the final 5 minutes.

Fixation: Cells were harvested at 4,000 x g for 5 minutes at 4°C, washed two times in 1 ml ice cold PBS with spins at 8,000 x g for 2 min at 4°C before being fixed with 4% paraformaldehyde in PBS for 30 minutes at room temperature. After fixation, cells were washed three times in PBS. For immunofluorescence the fixed cells were blocked overnight with 3% BSA in PBS at 4°C. Cells were harvested at 8,000 x g for 2 min at 4°C, resuspended in 1:500 Primary antibody (Mouse Anti-027 $SlpA_{R20291}$ LMW SLP) and incubated at room temperature for 1 hour. Cells were then washed three times in 1 ml 3% BSA in PBS before being resuspended in 1:500 secondary antibody (Goat anti-mouse-Cy5, Thermo Fisher). Cells were incubated for 1 hour at room temperature then washed three times in 3% BSA in PBS before being resuspended in PBS. Washed cells were dried down to glass cover slips and mounted with SlowFade Diamond (Thermo Fisher).

Images were taken on a Nikon Ti eclipse widefield imaging microscope using NIS elements software or a ZEISS LSM 880 with Airyscan using ZEN imaging software. Image J based FiJi was used for image analysis.

Cell Fractionation

Extracellular glycine preparation: Cells were harvested at 4,000 x g for 5 minutes at 4°C. In all the following wash steps bacterial cells we spun at 8,000 xg for 2 minutes. Pellets were washed twice by resuspension in 1 ml ice cold PBS. Cells were treated with 10 µl per $OD_{600}U$ of extraction buffer (0.2 M Glycine, pH 2.2) and incubated at room temperature for 30 minutes to strip extracellular proteins. Stripped cells were harvested and the supernatant, containing extracellular protein, was taken and neutralized with 0.15 µl 1.5 M Tris pH 8.8 per 1 µl extract. The stripped cells were washed twice in 1 ml ice cold PBS before being frozen at -80C. Cells were thawed and then resuspended in 11.5 µl per $OD_{600}U$ cell lysis buffer (PBS, 1x protease inhibitor cocktail, 5 mM EDTA, 20 ng/ml DNase, 120 mg/ml purified CD27L endolysin (Mayer, Garefalaki, Spoerl, Narbad, & Meijers, 2011)). Lysis was induced by incubating at 37°C shaking for 30 minutes. Cell membranes were harvested by centrifugation at 20,000 xg for 20 minutes and the soluble intracellular protein fraction retained before the pellet was

washed twice with 1 ml PBS. Membranes were solubilized using 11.5 µl per $D_{600}U$ solubilization buffer (1xPBS, 1x Protease Arrest, 5 mM EDTA, 20 ng/ml DNase, 1.5% sarkosyl) and agitated by rotating for 1 hour at room temperature. Insoluble material was harvested at 20,000 xg for 5 minutes and the solubilized membrane fraction was taken. Alternatively, for the SNAP tagged SlpA constructs; cells lysates were supplemented with 1.5% sarkosyl, incubated for 1 hour and harvested at 20,000 xg for 5 minutes to create a total cellular extract.

Protein Gels

Proteins were separated using standard SDS-PAGE techniques on a mini-protein III system (Bio-Rad) before being either; analyzed for in-gel florescence on a ChemiDoc imaging system (Bio-Rad), stained with Coomassie or transferred to nitrocellulose membranes using a semi-dry blotter (Bio-Rad) for western blot analysis. Band intensities were measured using Image Lab Software (Bio-Rad).

Statistics

Statistics were performed in Origin using one-way analysis of variance (ANOVA), a difference with $p \leq 0.05$ was considered significant.

Acknowledgements

We would like to thank Darren Robinson and Christa Walther at The Wolfson Light Microscopy Facility at the University of Sheffield for their help with microscopy.

This work was supported by the Medical Research Council (grant number MR/N000900/1) and the Wellcome Trust (grant number 204877/Z/16/Z).

References

Arkowitz, R. A., Joly, J. C., & Wickner, W. (1993). Translocation can drive the unfolding of a preprotein domain. *EMBO J, 12*(1), 243-253.

Bensing, B. A., Seepersaud, R., Yen, Y. T., & Sullam, P. M. (2014). Selective transport by SecA2: an expanding family of customized motor proteins. *Biochim Biophys Acta, 1843*(8), 1674-1686. doi:10.1016/j.bbamcr.2013.10.019

Bonardi, F., Halza, E., Walko, M., Du Plessis, F., Nouwen, N., Feringa, B. L., & Driessen, A. J. (2011). Probing the SecYEG translocation pore size with preproteins conjugated with sizable rigid spherical molecules. *Proc Natl Acad Sci U S A, 108*(19), 7775-7780. doi:10.1073/pnas.1101705108

Cartman, S. T., Kelly, M. L., Heeg, D., Heap, J. T., & Minton, N. P. (2012). Precise manipulation of the Clostridium difficile chromosome reveals a lack of association between the tcdC genotype and toxin production. *Appl Environ Microbiol, 78*(13), 4683-4690. doi:10.1128/AEM.00249-12

Colavin, A., Shi, H., & Huang, K. C. (2018). RodZ modulates geometric localization of the bacterial actin MreB to regulate cell shape. *Nat Commun, 9*(1), 1280. doi:10.1038/s41467-018-03633-x

de la Riva, L., Willing, S. E., Tate, E. W., & Fairweather, N. F. (2011). Roles of cysteine proteases Cwp84 and Cwp13 in biogenesis of the cell wall of Clostridium difficile. *J Bacteriol, 193*(13), 3276-3285. doi:10.1128/JB.00248-11

Dembek, M., Barquist, L., Boinett, C. J., Cain, A. K., Mayho, M., Lawley, T. D., . . . Fagan, R. P. (2015). High-throughput analysis of gene essentiality and sporulation in Clostridium difficile. *MBio, 6*(2), e02383. doi:10.1128/mBio.02383-14

Eilers, M., & Schatz, G. (1986). Binding of a specific ligand inhibits import of a purified precursor protein into mitochondria. *Nature, 322*(6076), 228-232. doi:10.1038/322228a0

Fagan, R. P., & Fairweather, N. F. (2011). Clostridium difficile has two parallel and essential Sec secretion systems. *J Biol Chem, 286*(31), 27483-27493. doi:10.1074/jbc.M111.263889

Fagan, R. P., & Fairweather, N. F. (2014). Biogenesis and functions of bacterial S-layers. *Nat Rev Microbiol, 12*(3), 211-222. doi:10.1038/nrmicro3213

Greaves, N. S., Ashcroft, K. J., Baguneid, M., & Bayat, A. (2013). Current understanding of molecular and cellular mechanisms in fibroplasia and angiogenesis during acute wound healing. *J Dermatol Sci, 72*(3), 206-217. doi:10.1016/j.jdermsci.2013.07.008

Hull, M. W., & Beck, P. L. (2004). Clostridium difficile-associated colitis. *Can Fam Physician, 50*, 1536-1540, 1543-1535.

Kim, J., & Kendall, D. A. (2000). Sec-dependent protein export and the involvement of the molecular chaperone SecB. *Cell Stress Chaperones, 5*(4), 267-275.

Kirby, J. M., Ahern, H., Roberts, A. K., Kumar, V., Freeman, Z., Acharya, K. R., & Shone, C. C. (2009). Cwp84, a surface-associated cysteine protease, plays a role in the maturation of the surface layer of Clostridium difficile. *J Biol Chem, 284*(50), 34666-34673. doi:10.1074/jbc.M109.051177

Kirk, J. A., & Fagan, R. P. (2016). Heat shock increases conjugation efficiency in Clostridium difficile. *Anaerobe, 42*, 1-5. doi:10.1016/j.anaerobe.2016.06.009

Kirk, J. A., Gebhart, D., Buckley, A. M., Lok, S., Scholl, D., Douce, G. R., . . . Fagan, R. P. (2017). New class of precision antimicrobials redefines role of Clostridium difficile S-layer in virulence and viability. *Sci Transl Med, 9*(406). doi:10.1126/scitranslmed.aah6813

Kuru, E., Hughes, H. V., Brown, P. J., Hall, E., Tekkam, S., Cava, F., . . . VanNieuwenhze, M. S. (2012). In Situ probing of newly synthesized peptidoglycan in live bacteria with fluorescent D-amino acids. *Angew Chem Int Ed Engl, 51*(50), 12519-12523. doi:10.1002/anie.201206749

Mayer, M. J., Garefalaki, V., Spoerl, R., Narbad, A., & Meijers, R. (2011). Structure-based modification of a Clostridium difficile-targeting endolysin affects activity and host range. *J Bacteriol, 193*(19), 5477-5486. doi:10.1128/JB.00439-11

McNeil, P. L., & Baker, M. M. (2001). Cell surface events during resealing visualized by scanning-electron microscopy. *Cell Tissue Res, 304*(1), 141-146.

Merrigan, M. M., Venugopal, A., Roxas, J. L., Anwar, F., Mallozzi, M. J., Roxas, B. A., . . . Vedantam, G. (2013). Surface-layer protein A (SlpA) is a major contributor to host-cell adherence of Clostridium difficile. *PLoS One, 8*(11), e78404. doi:10.1371/journal.pone.0078404

Mescher, M. F., & Strominger, J. L. (1976). Structural (shape-maintaining) role of the cell surface glycoprotein of Halobacterium salinarium. *Proc Natl Acad Sci U S A, 73*(8), 2687-2691.

Monot, M., Boursaux-Eude, C., Thibonnier, M., Vallenet, D., Moszer, I., Medigue, C., . . . Dupuy, B. (2011). Reannotation of the genome sequence of Clostridium difficile strain 630. *J Med Microbiol, 60*(Pt 8), 1193-1199. doi:10.1099/jmm.0.030452-0

Napolitano, L. M., & Edmiston, C. E., Jr. (2017). Clostridium difficile disease: Diagnosis, pathogenesis, and treatment update. *Surgery, 162*(2), 325-348. doi:10.1016/j.surg.2017.01.018

Ransom, E. M., Ellermeier, C. D., & Weiss, D. S. (2015). Use of mCherry Red fluorescent protein for studies of protein localization and gene expression in Clostridium difficile. *Appl Environ Microbiol, 81*(5), 1652-1660. doi:10.1128/AEM.03446-14

Rassow, J., Guiard, B., Wienhues, U., Herzog, V., Hartl, F. U., & Neupert, W. (1989). Translocation arrest by reversible folding of a precursor protein imported into mitochondria. A means to quantitate translocation contact sites. *J Cell Biol, 109*(4 Pt 1), 1421-1428.

Takumi, K., Koga, T., Oka, T., & Endo, Y. (1991). Self-Assembly, Adhesion, And Chemical Properties Of Tetragonarly Arrayed S-Layer Proteins Of *Clostridium*. *The Journal of General and Applied Microbiology, 37*(6), 455-465. doi:10.2323/jgam.37.455

Tang, S. K. Y., & Marshall, W. F. (2017). Self-repairing cells: How single cells heal membrane ruptures and restore lost structures. *Science, 356*(6342), 1022-1025. doi:10.1126/science.aam6496

Willing, S. E., Candela, T., Shaw, H. A., Seager, Z., Mesnage, S., Fagan, R. P., & Fairweather, N. F. (2015). Clostridium difficile surface proteins are anchored to the cell wall using CWB2 motifs that recognise the anionic polymer PSII. *Mol Microbiol, 96*(3), 596-608. doi:10.1111/mmi.12958

Wright, A., Wait, R., Begum, S., Crossett, B., Nagy, J., Brown, K., & Fairweather, N. (2005). Proteomic analysis of cell surface proteins from Clostridium difficile. *Proteomics, 5*(9), 2443-2452. doi:10.1002/pmic.200401179

Main Figure Legends

Figure 1: Schematic diagram of the *C. difficile* S-layer and the SlpA secretory pathway.

A: Domain structure of SlpA precursor protein with signal sequence (Pink), low molecular weight region (LMW, Red) and high molecular weight region (HMW, Blue) that contains three cell wall binding domains (CWB, 1-3 in Grey).

B: Schematic diagram of SlpA secretion and processing in *C. difficile*. SlpA (Pink/Red/blue line) is translated in the cytosol (light green) and targeted for secretion across the membrane using SecA2 (Purple oval) most likely via the SecYEG Channel (Yellow/Orange). Cwp84 (Scissors) cleaves SlpA into low molecular weight (LMW, Red spheres) and high molecular weight (HMW, Blue spheres) S-layer protein (SLP) subunits. The HMW and LMW SLPs assemble to form hetero-dimers that incorporate into the S-layer. The surface of the S-layer consists largely of exposed LWM SLP anchored to the cell wall (light blue) via cell wall biding domains of the HMW component (see A).

C: Models of SlpA integration into the S-layer. (i) unfolded SlpA (red line) is secreted from specific points on the cell membrane - directed by gaps in the S-layer or cell wall (colored as in Figure 1B), newly processed SlpA (LMW orange circles, HMW light blue ovals) is transported directly through the cell wall for integration into the S-layer. Alternatively; (ii) SlpA is translocated across the cell membrane at multiple sites. A pool of SlpA lays within the cell wall ready to fill gaps in the S-layer.

Figure 2: New surface S-layer colocalizes with areas of new peptidoglycan synthesis.

A: Airyscan confocal image of a *C. difficile* 630 cell grown with HADA to label peptidoglycan cell wall (Blue) and chased to reveal darker areas of newly synthesized cell wall. This chase was followed by a short expression of $SlpA_{R20291}$ which was specifically immunolabeled with Cy5 (White). Yellow bar indicates the region used for the intensity plot in B. Scale bar indicates 3 µm.

B: Intensity plot depicting signal from HADA (Blue) and Cy5 (Grey) along the yellow bar illustrated in A.

Figure 3: S-layer formation during cell division.

Airyscan confocal images of *C. difficile* 630 cells during and immediately after cell division with HADA labelled peptidoglycan cell wall (blue) and new surface $SlpA_{R20291}$ immunolabeled with Cy5 (white). Large, dark areas lacking HADA staining mark cell wall synthesis at the septum between cells or a newly produced cell pole. Scale bar indicates 3 µm. On the right-hand side of each row is a schematic diagram illustrating the position of new surface $SlpA_{R20291}$ (HMW SLP, spotted light blue and LMW SLP, spotted orange) as detected in the corresponding microscopy images against the position of endogenous surface $SlpA_{630}$ (HMW SLP, dark blue and LMW SLP, red). The position of newly synthesized cell wall is displayed in brown/white stripes.

Figure 4: SecA2-SNAP localization and new S-layer.

A: Widefield phase contrast (left panels) and fluorescent (right panels) images of wild type *C. difficile* 630 or 630 *secA2-snap* cells stained with TMR-Star (red). Scale bar indicates 3 µm.

B: Airyscan confocal image displaying SecA2-SNAP-TMR-Star signal distribution in *C. difficile* 630 cells. Scale bar indicates 3 µm.

C: Airyscan confocal image showing the localization of SecA2-SNAP-TMR-Star (red) in relation to the synthesis of cell wall (dark patches lacking blue HADA stain) and newly synthesized S-layer (Cy5, white). Scale bar indicates 3 µm.

Figure 5: Sites of S-layer secretion.

A: Schematic diagram of SlpA-SNAP (left panel) and SlpA-DHFR-SNAP (right panel) in *C. difficile* 630 cells (colored as in Figure 1B) with SNAP tags represented as an orange coil. SlpA-SNAP is exported and cleaved into LMW SLP and HMW SLP-SNAP which can bind TMR-Star. The DHFR domain (dark gray oval) of SlpA-DHFR-SNAP blocks the translocon channel during export, leaving the TMR-Star bound SNAP tag in the cytosol.

B: Widefield phase contrast (left panels) and fluorescent TMR-Star signal (right panels) of *C. difficile* 630 cells imaged with and without induction of SlpA-SNAP expression.

C: Overlay of signal in the induced sample (from B) with areas taken for the plot profiles labelled (yellow lines, i-iii).

D: SlpA-SNAP profile plots of i-iii (from **C**) of phase contrast signal (black) and TMR-Star signal (red).

E: SlpA-DHFR-SNAP in *C. difficile* 630 cells (labelled as in **B**).

F: Overlay of signal in the induced sample (from **E**, labelled as in **C**).

G: SlpA-DHFR-SNAP profile plots of i-iii (from **F**) (Labelled as in **D**).

Figure 6: Model of S-layer in the cell wall.

Schematic flow diagram of SlpA secretion and S-layer formation (colored as in Figure 1C). During normal cell growth SlpA is targeted by SecA2 for secretion all over the cytosolic membrane. A store of SlpA resides within the cell wall where it is processed ready for integration into the S-layer (i). Gaps may form in the S-layer due to cell growth or injury (ii). SlpA in the cell wall diffuses out (iii) and fills openings in the S-layer (iv).

Supplemental Figure Legends

Figure 2S1: *C. difficile* 630 HADA staining chase time course

A: Widefield microscopy displaying phase contrast (upper panels) and fluorescence (lower panels) of HADA stained *C. difficile* 630 cells chased for 0, 10, 20 or 30 min without HADA (as described in Methods). HADA staining at the center of a dividing cell can be characterized as: septum stained (left) or patches of reduced HADA staining being smaller than 360 nm in length (middle) or larger (right).

B: Graph displaying the population distribution of dividing *C. difficile* 630 cells characterized for HADA staining in widefield microscopy (as in Figure 2S1A) when chased for HADA for 0, 10, 20 or 30 minutes (T0, n=56; T10, n=62; T20, n=71; T30, n=107). The percentage of the total counted population are displayed above each bar.

Figure 2S2: Antibody specificity for SlpA$_{R20291}$ LMW SLP.

A: Top panel: Coomassie stain of SDS-PAGE separated extracellular extracts from *C. difficile* 630 cells grown for three hours with the indicated amount of anhydrotetracycline (Atc) to induce protein expression. Lower panel: Western immunoblot to detect SlpA$_{R20291}$ LMW SLP in the same extracellular extracts.

B: Widefield microscopy of *C. difficile* 630 cells with pRPF238 (encoding SlpA$_{R20291}$::LMW-Tetracysteine. The tetracysteine (Tc) tag was used during other labelling experiments that were unsuccessful (data not shown)) induced (bottom panels) or not induced (top panels) with 100 ng/ml Atc for 5 minutes. Surface SlpA$_{R20291}$ was immunolabeled with Cy5 (magenta). Scale bar indicates 6 µm.

Figure 2S3: Further images of new surface S-layer

Further examples of airyscan confocal images displaying *C. difficile* 630 cells prepared as in Figure 2 with HADA label peptidoglycan cell wall (Blue), new SlpA$_{R20291}$ immunolabeled with Cy5 (White) and yellow bar regions used for intensity plot graphs. Intensity plot graphs display HADA (Blue) and Cy5 (Grey) signal with upper and lower graphs corresponding to the higher and lower cell region marked with yellow bars in the left panels, respectively.

Figure 4S1: SecA2-SNAP is functional in *C. difficile.*

A: Western immunoblot showing the distribution of SecA2 in extracellular (E), cytosolic (C) and membrane (M) fractions from wild-type *C. difficile* 630 or cells expressing a genomic copy of a *secA2-SNAP* fusion, loaded at the same OD_{600}U.

B: In-gel fluorescence of SecA2-SNAP-TMR-Star from cell extracts expressing SecA2-SNAP (labelled as in A).

C: Growth curves of wild-type *C. difficile* 630 (wt) or 630 *secA2-SNAP*. Following inoculation at an OD_{600} of 0.05, growth was followed by measuring OD_{600} hourly. Shown are the mean and standard error of duplicate cultures.

Figure 5S1: SlpA-SNAP, SlpA-DHFR-SNAP, SlpA-DHFR expression and localization

A: Fluorescence displaying SNAP- TMR-Star signal from extracellular (E) or cellular (C) *C. difficile* 630 extracts expressing SlpA-SNAP or SlpA-DHFR-SNAP.

B: SDS PAGE analysis of extracellular extracts stained with coomassie (upper panel) or membrane fractions analyzed by Western immunoblot with an anti-strep-tag antibody (lower panel) from *C. difficile* 630 cells expressing full length SlpA-DHFR or SlpA-DHFR lacking a signal sequence (ΔSS). Protein expression was induced with 20 ng/ml Atc for 180 min as indicated.

Figure 5S2: Characterization of a SlpA-DHFR fusion protein

A: Western immunoblot analysis of *C. difficile* R20291 expressing an SlpA-DHFR-3xHA fusion. Protein expression was induced (+) with 20 ng/ml Atc for 1 hour and intracellular cell extracts (membrane and cytosol) were analyzed by SDS PAGE followed by Western immunoblot using an anti-HA antibody to show expression of SlpA-DHFR-3xHA (top panel), anti-$SlpA_{R20291}$ to visualize accumulation of native SlpA precursor in the cytosol (middle panel) and anti-AtpB as a membrane protein and loading control (bottom panel). Samples from triplicate cultures are shown.

B: Quantification of average fold change of intracellular $SlpA_{R20291}$ precursor band intensity from A. Native $SlpA_{R20291}$ secretion is blocked by expression of SlpA-DHFR-3xHA. Asterisk indicates a significant difference ($p \leq 0.05$).

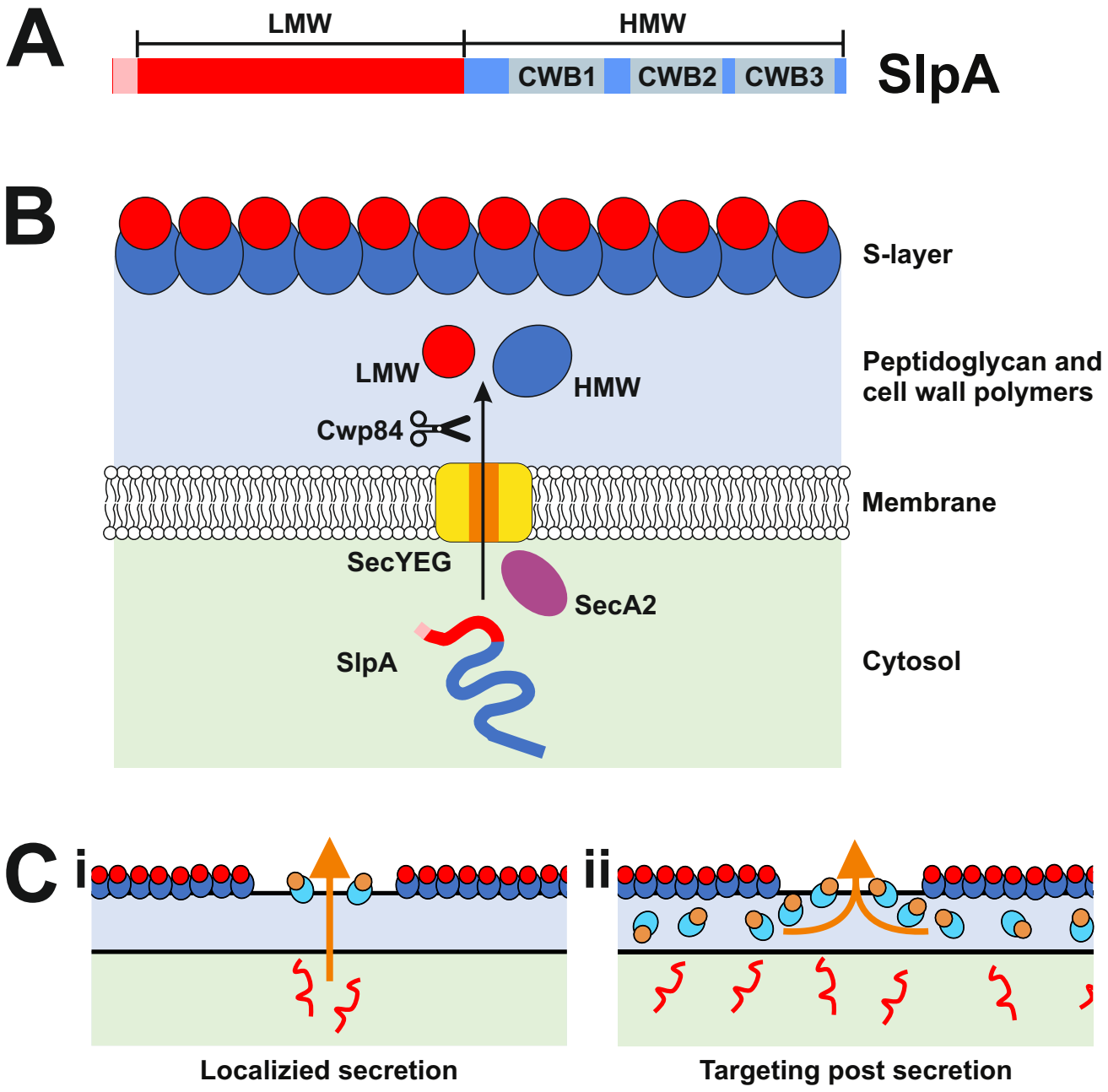

Figure 1

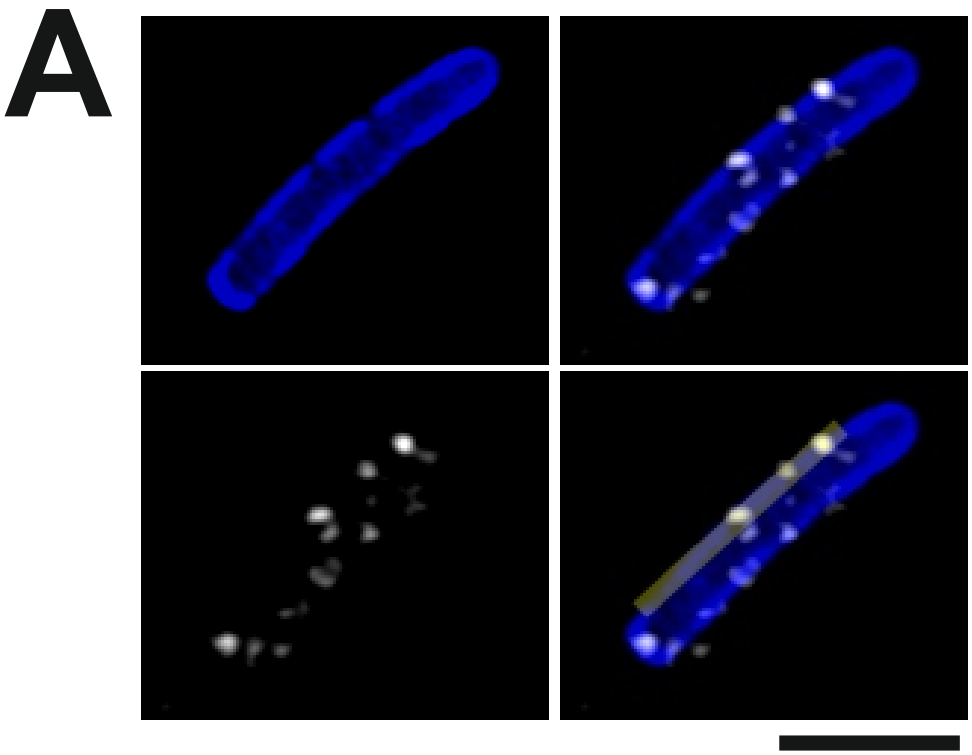

Figure 2

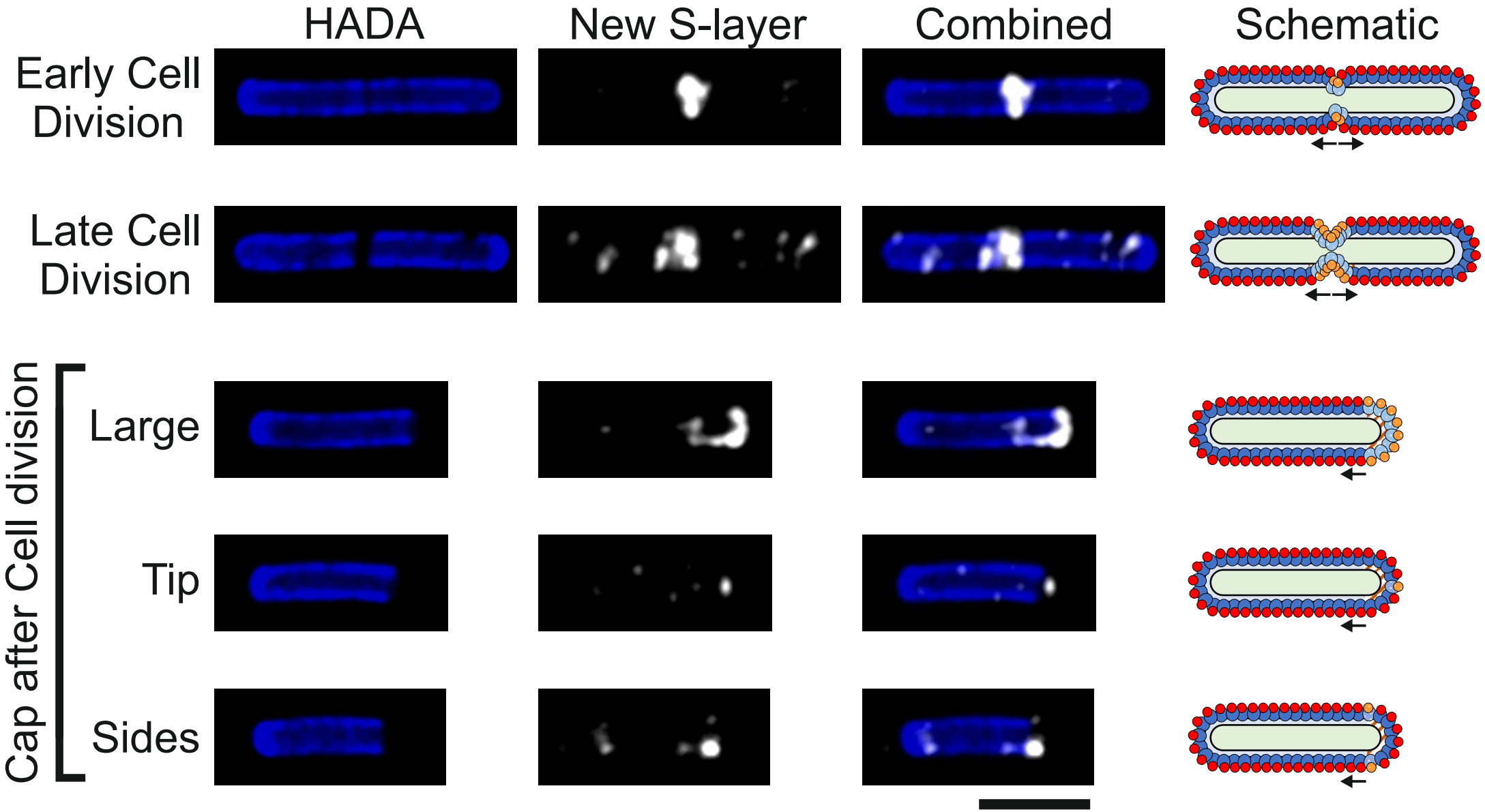
HADA
New S-layer
Combined
Schematic
Early Cell Division
Late Cell Division
Cap after Cell division
Large
Tip
Sides

Figure 3

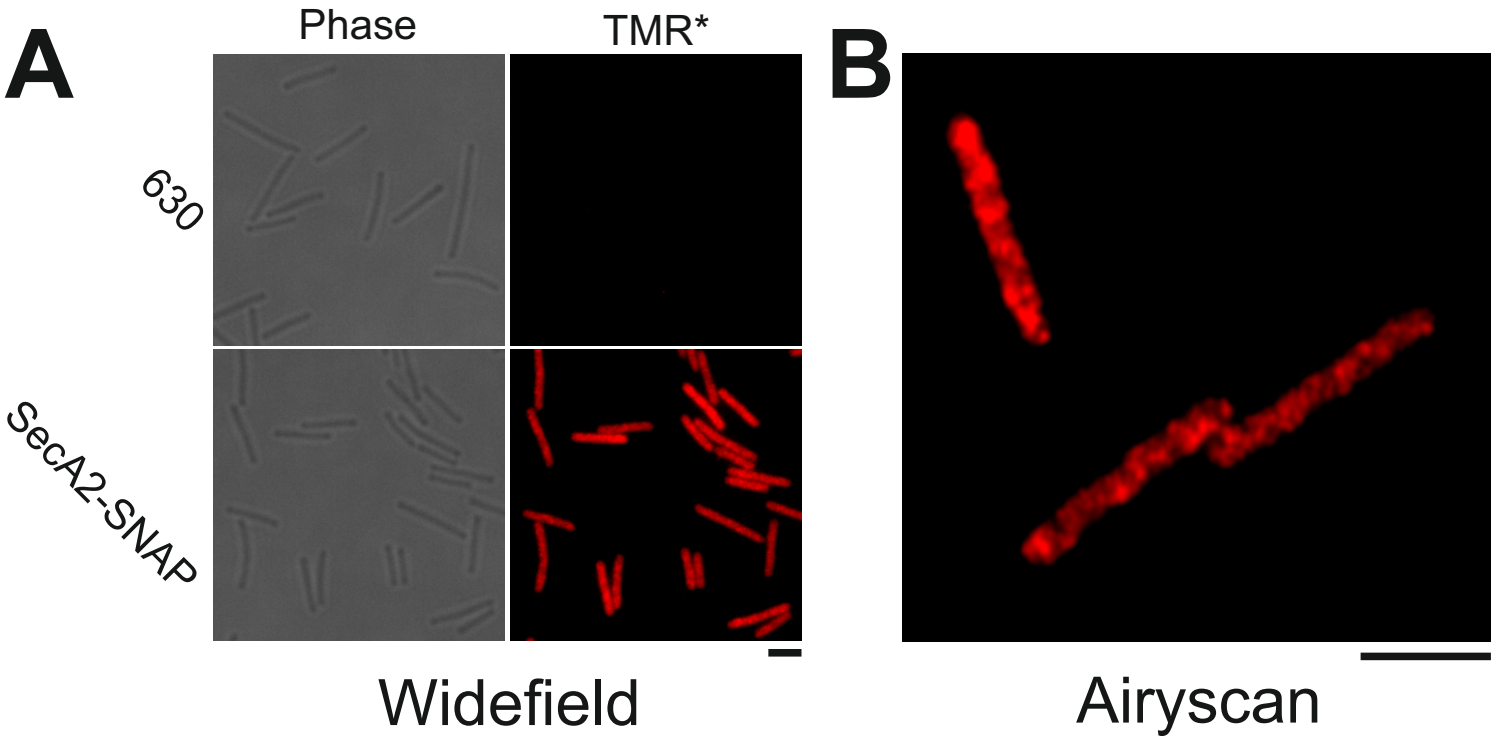

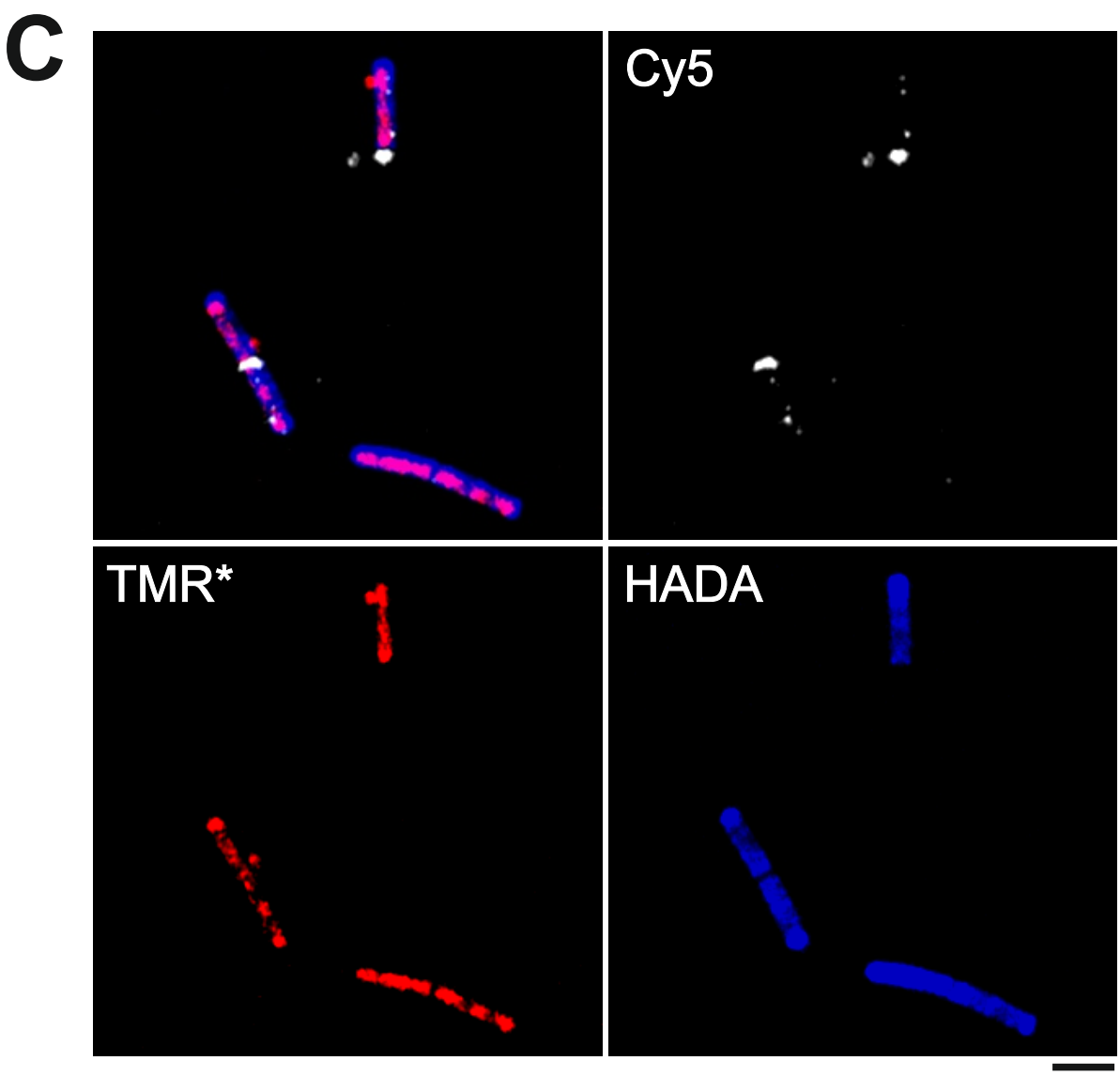

Figure 4

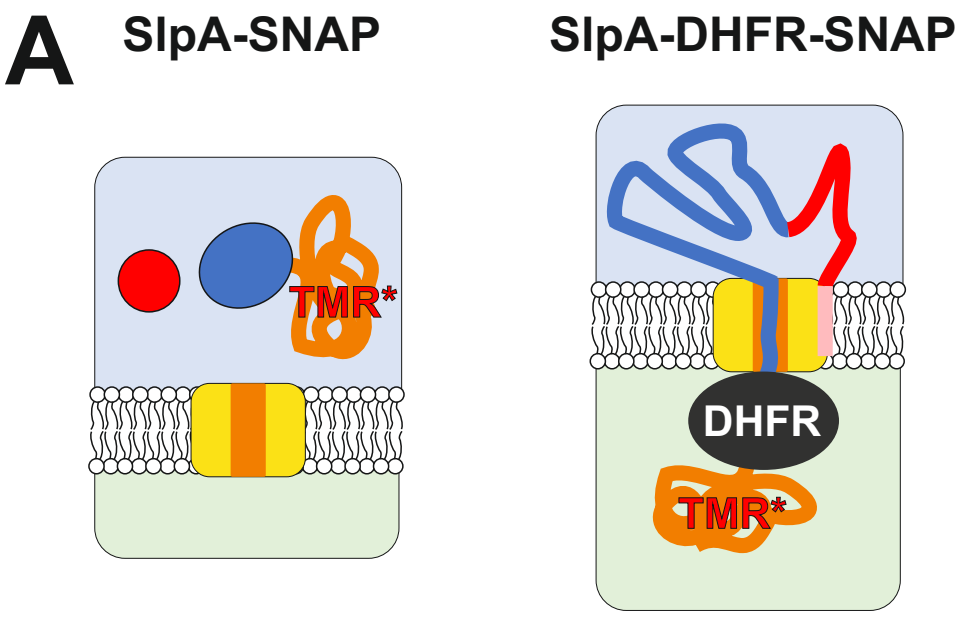

Figure 5A

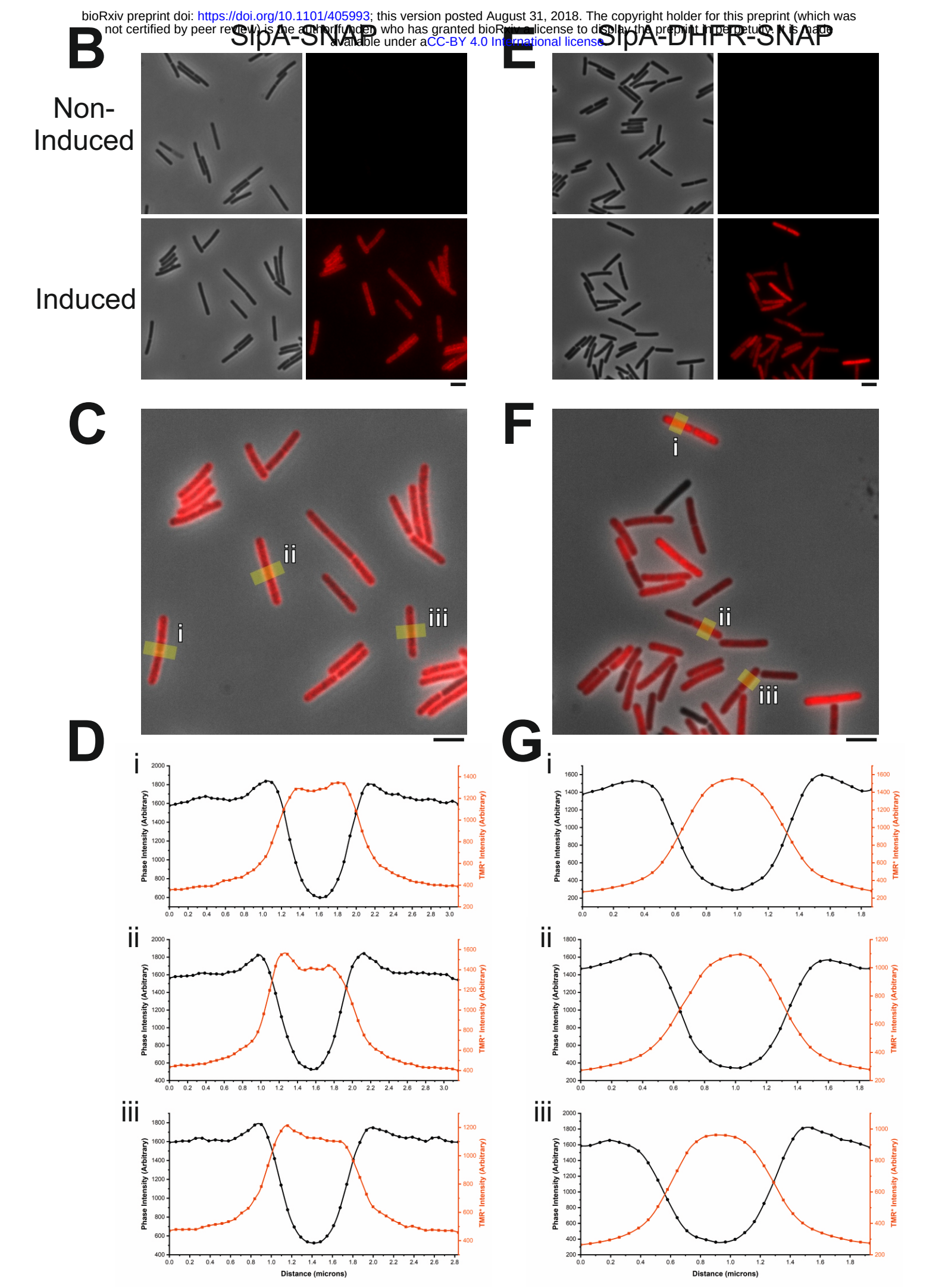

Figure 5B-G

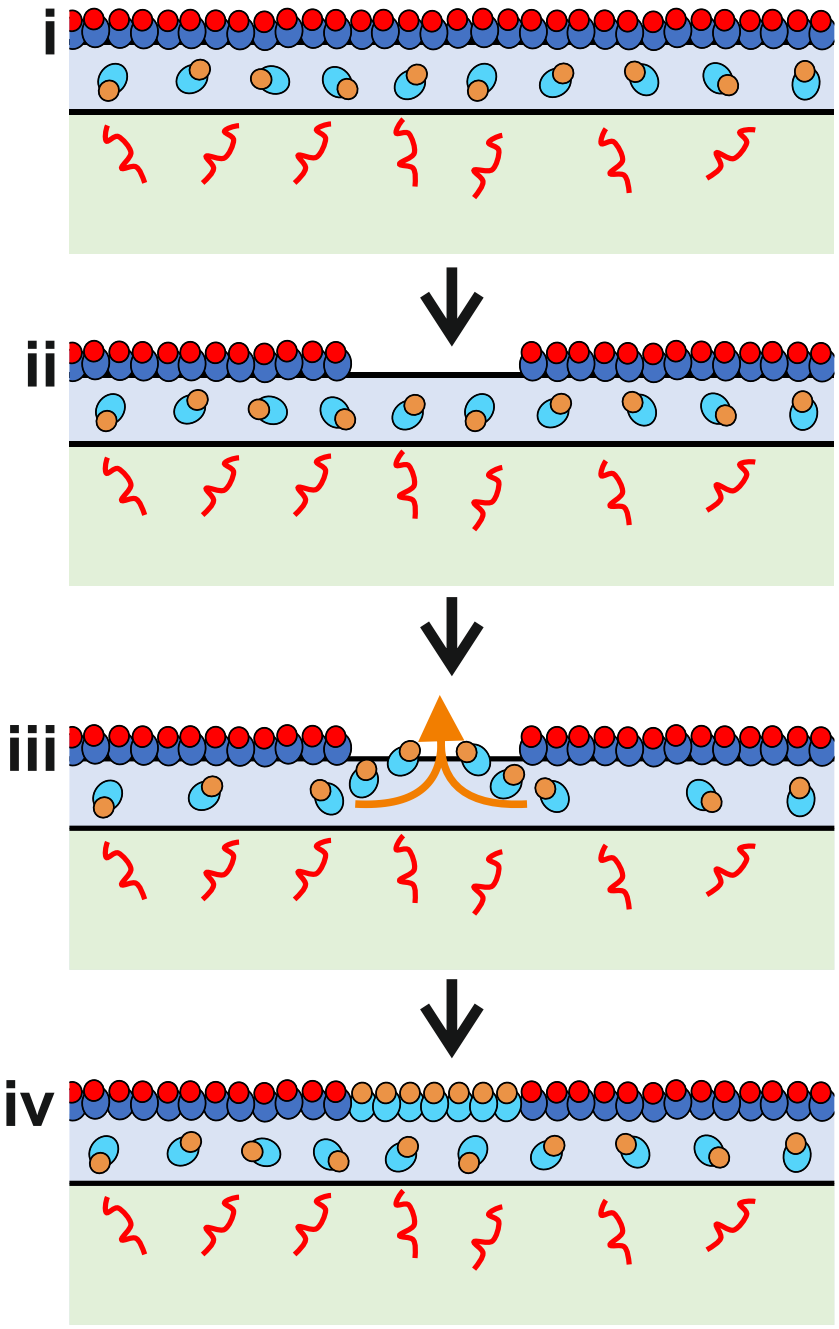

Pool of SlpA resides within the cell wall.

A gap Froms in S-layer (cell growth or disruption).

SlpA migrates from the cell wall to fill gaps in the S-layer.

New S-layer is formed.

Figure 6

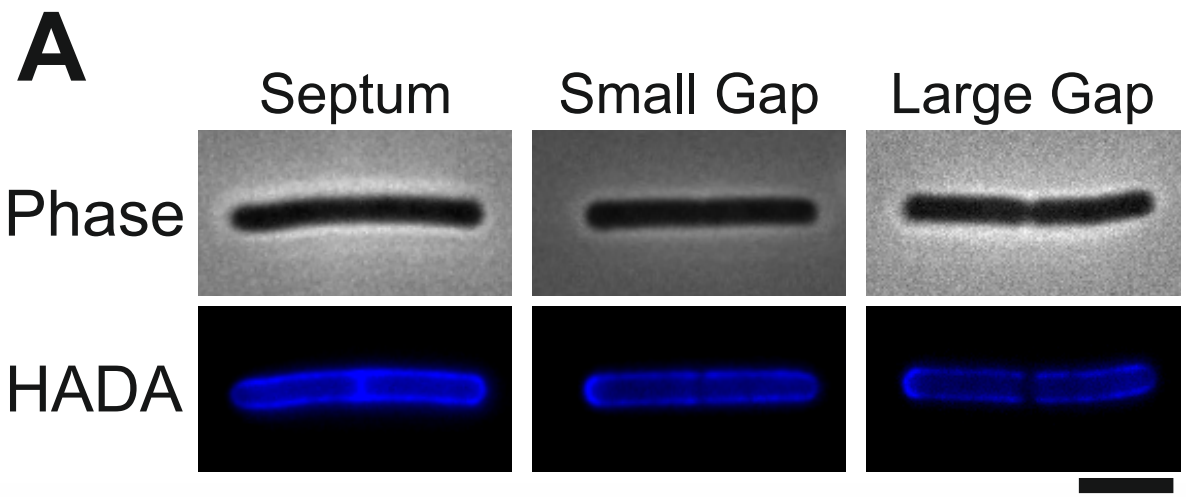

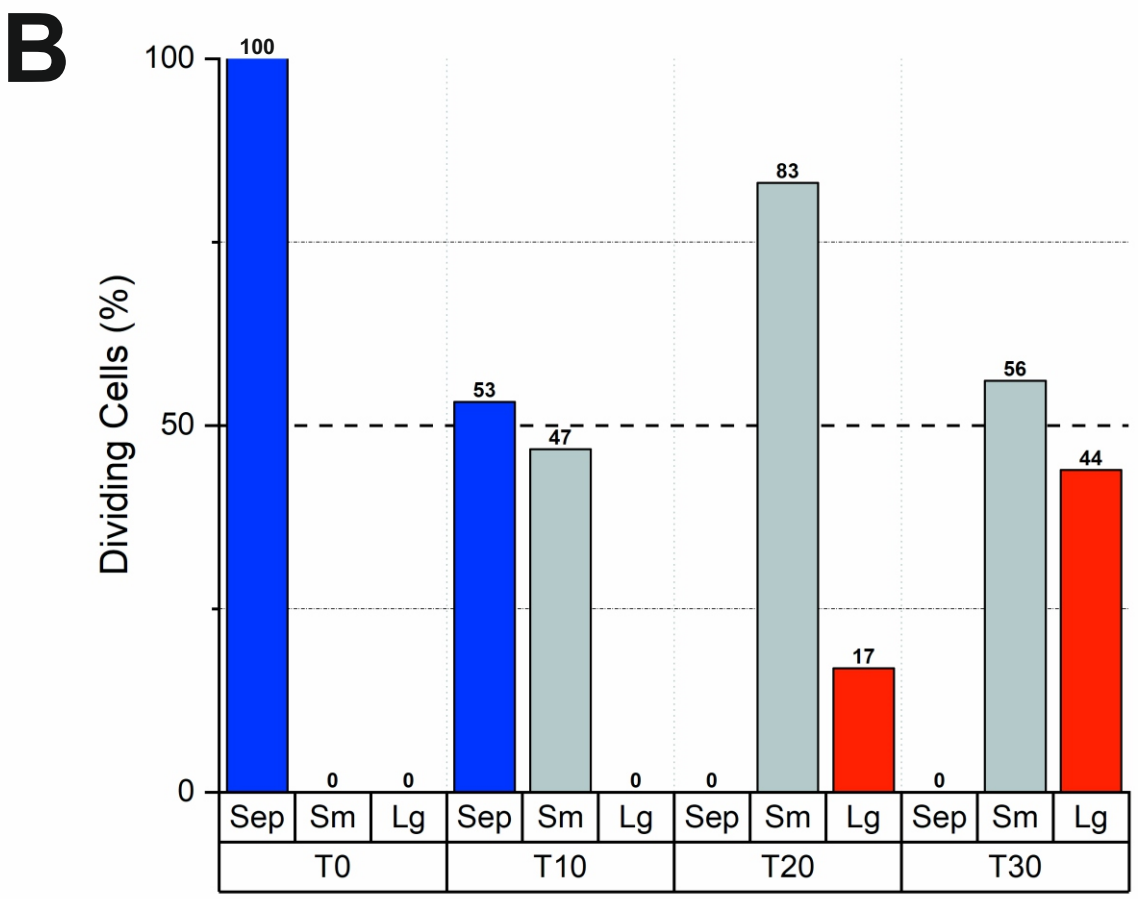

Supplementary Figure 2S1

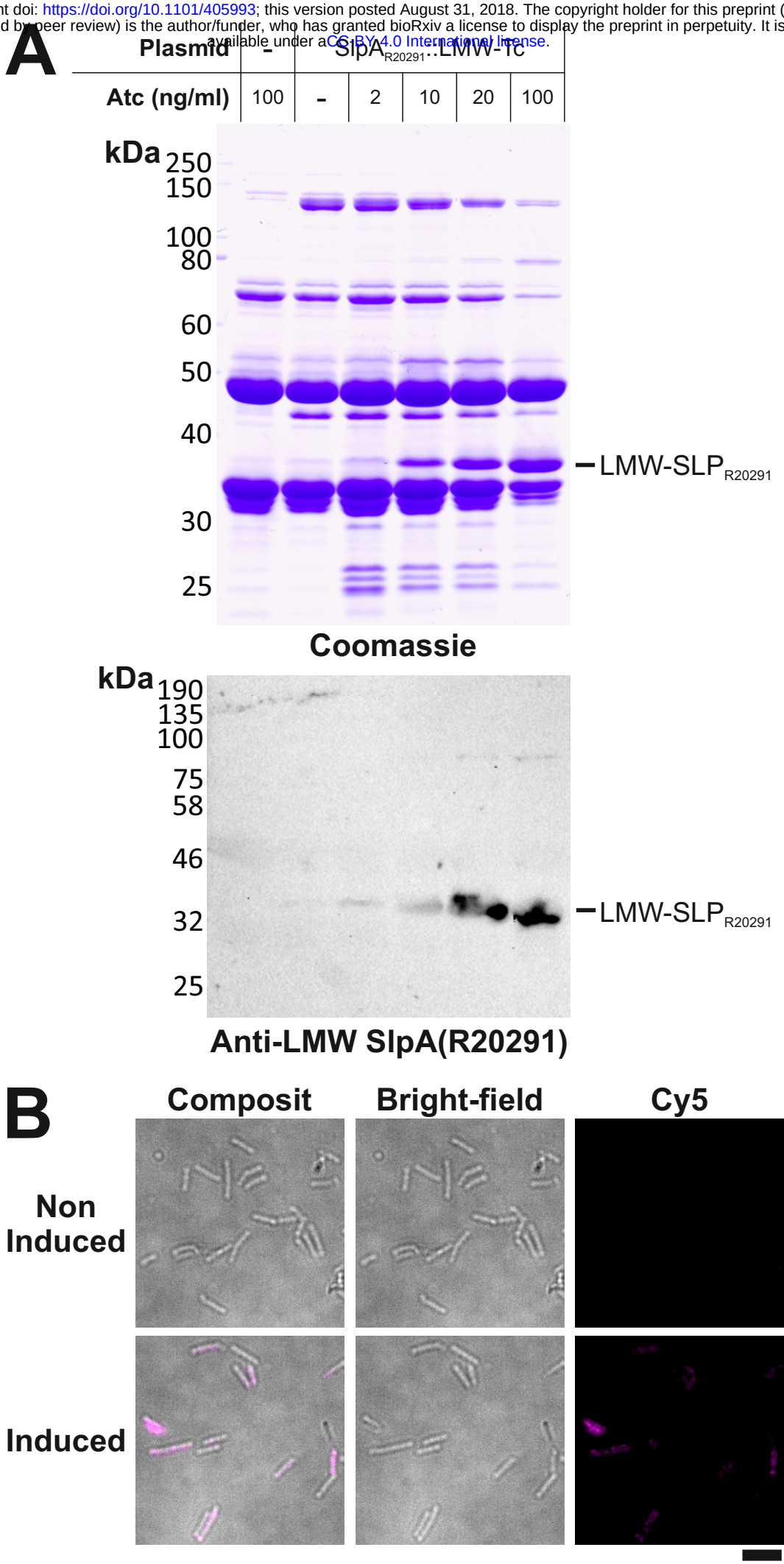

Supplementary Figure 2S2

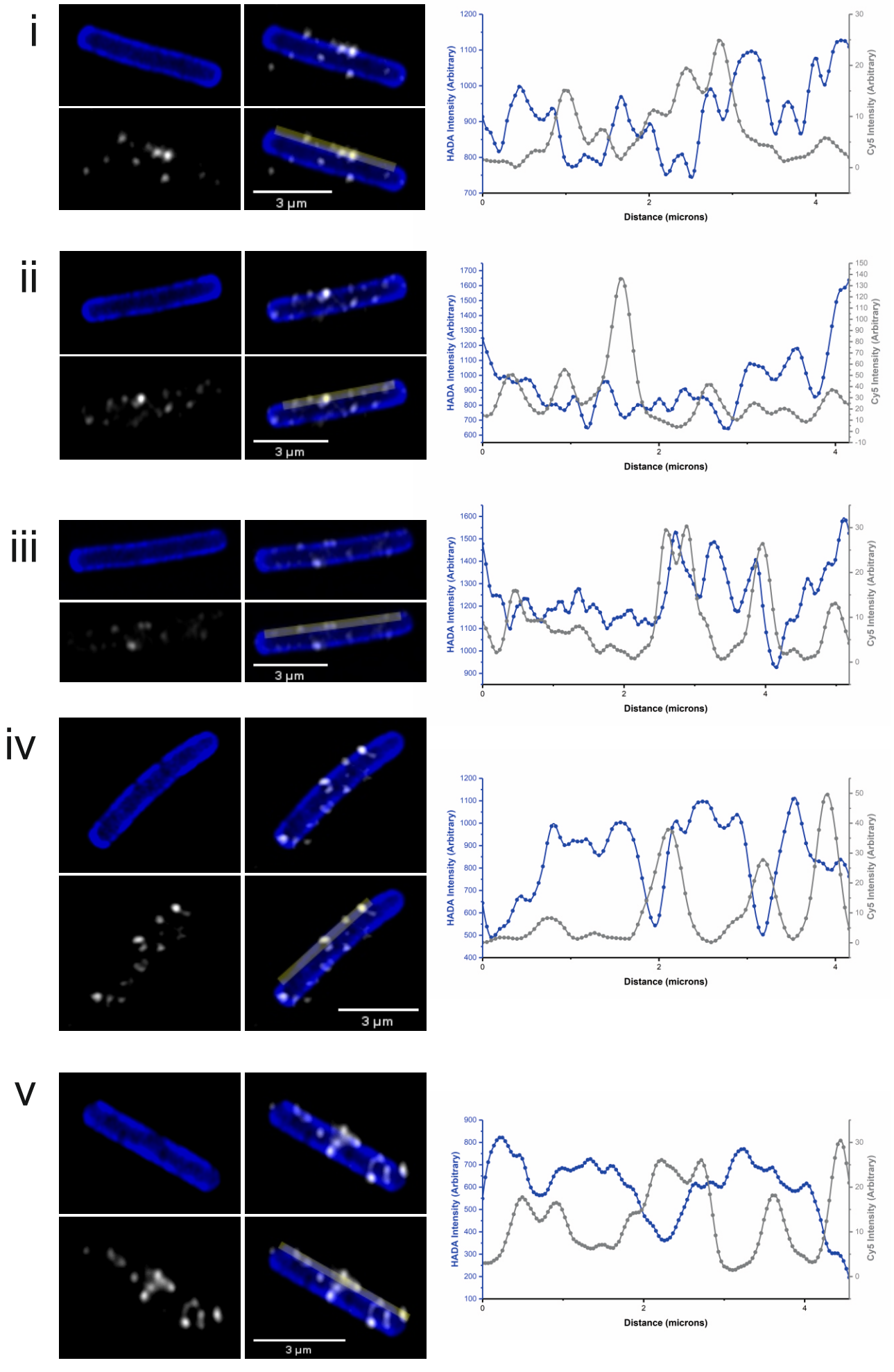

Supplementary Figure 2S3a

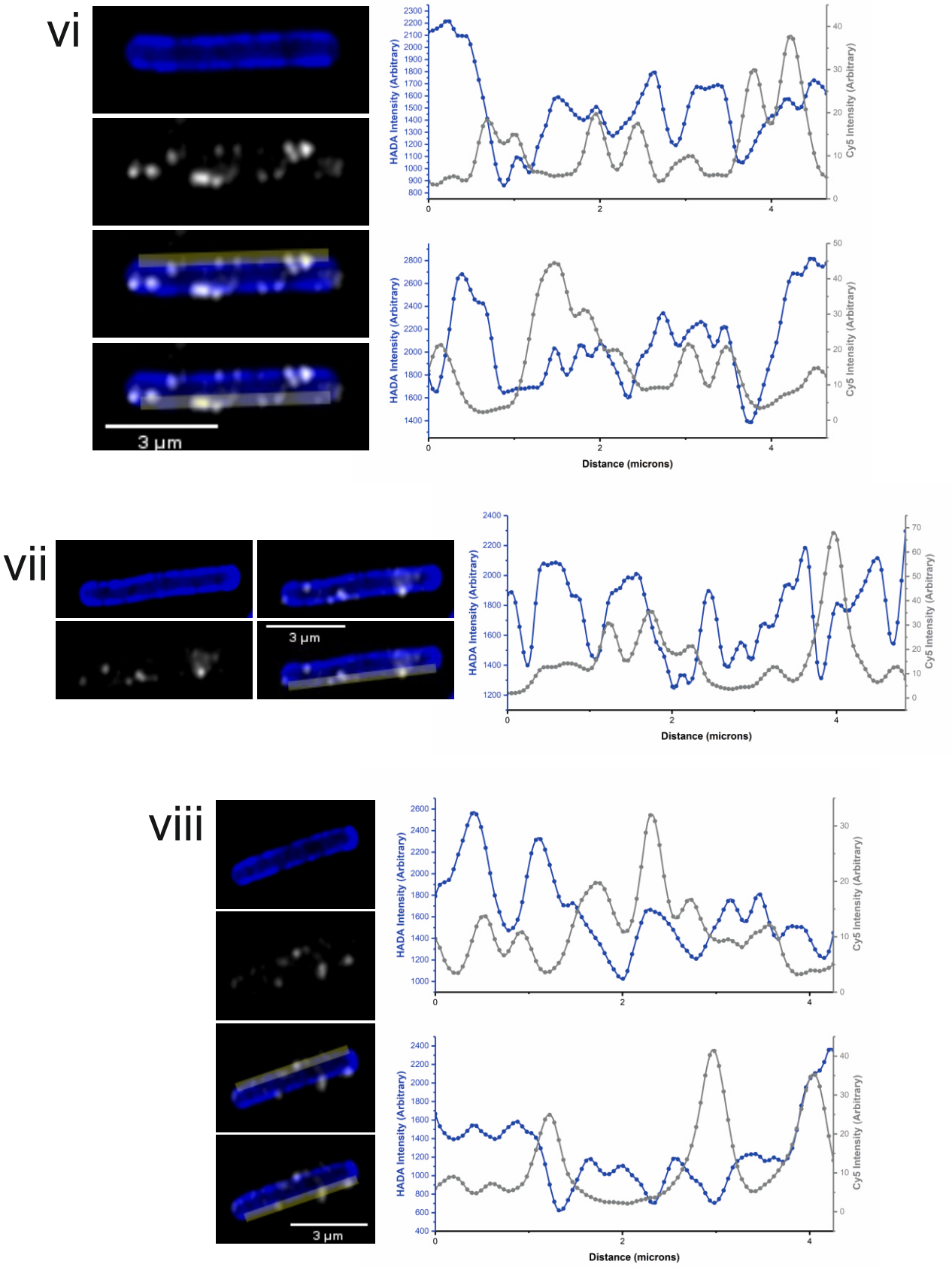

Supplementary Figure 2S3b

iX

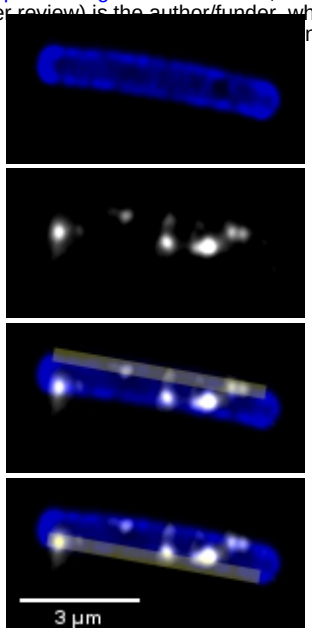

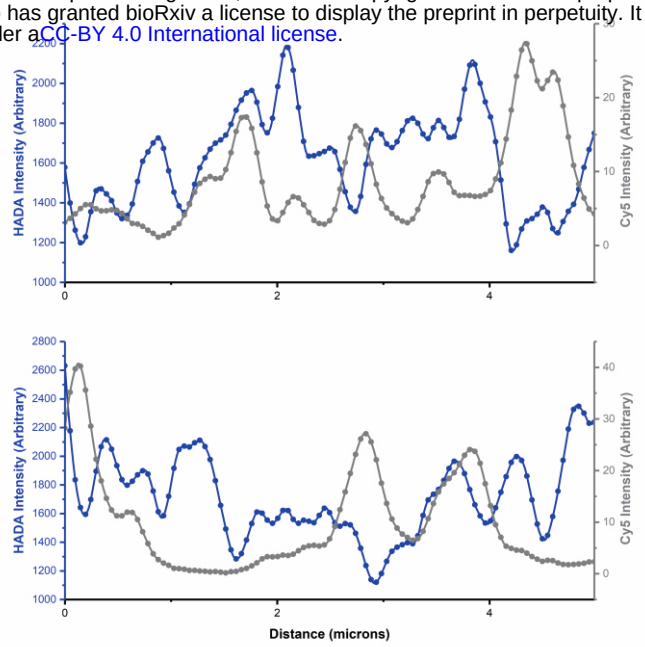

X

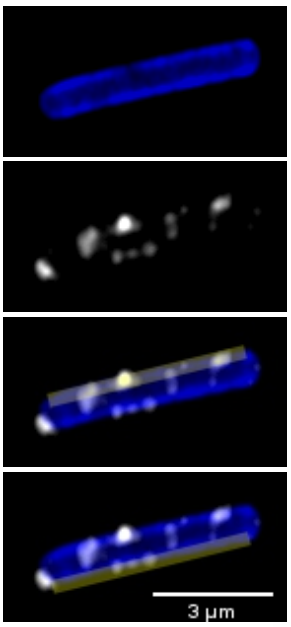

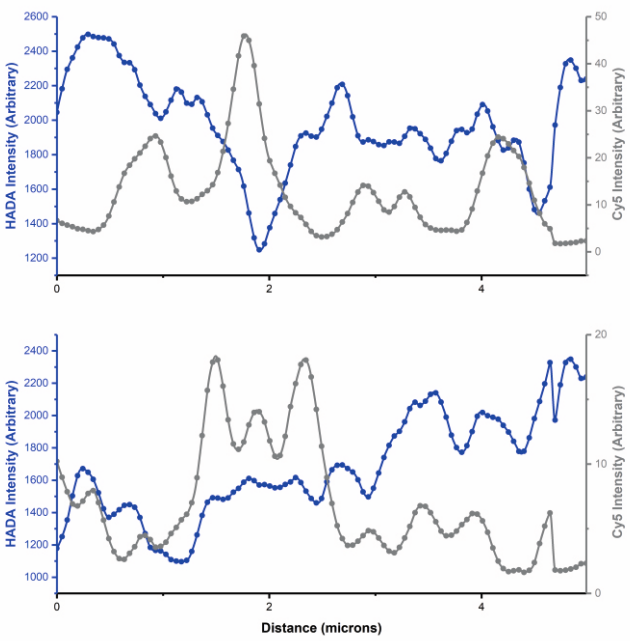

Xi

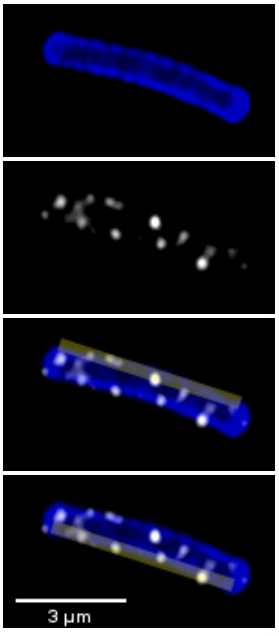

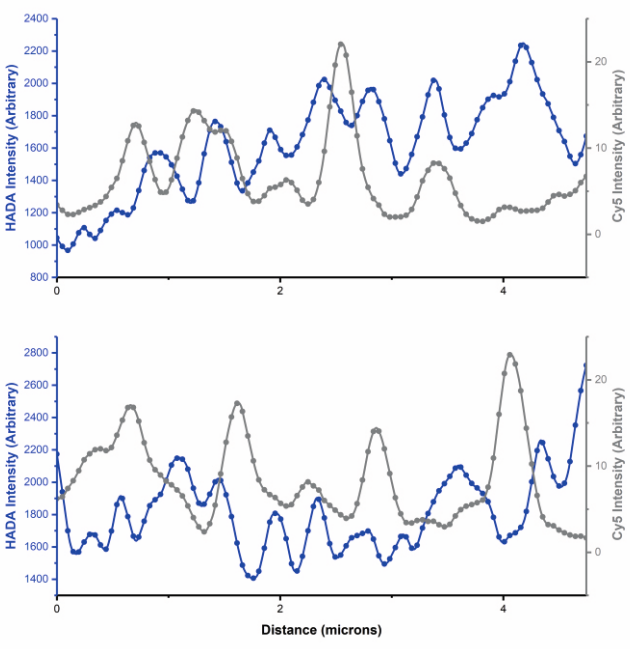

Supplementary Figure 2S3c

Xii

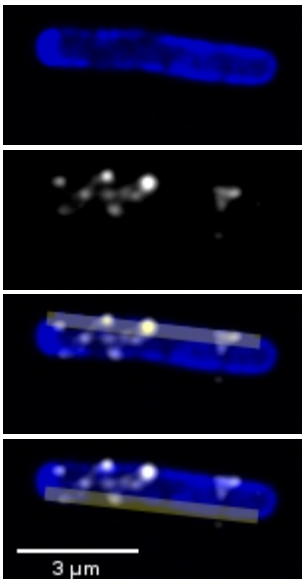

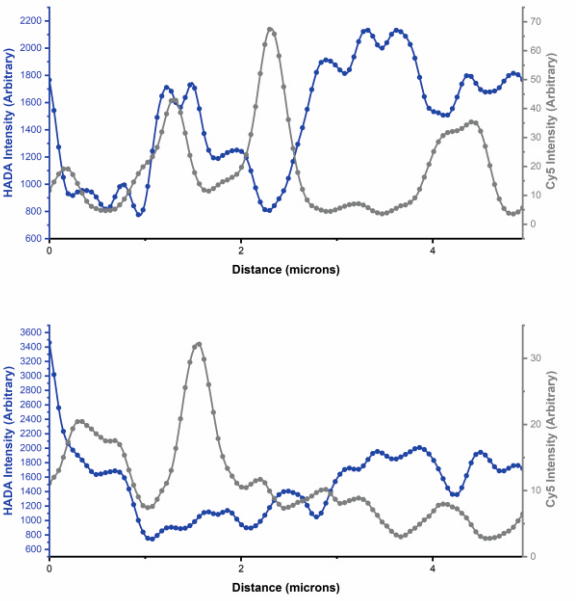

Xiii

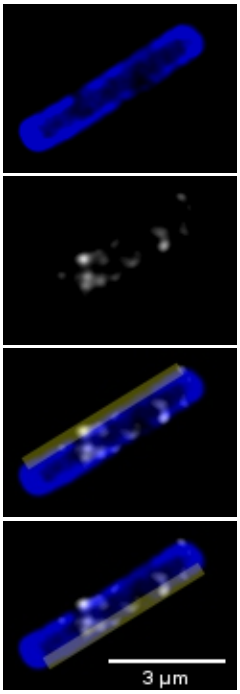

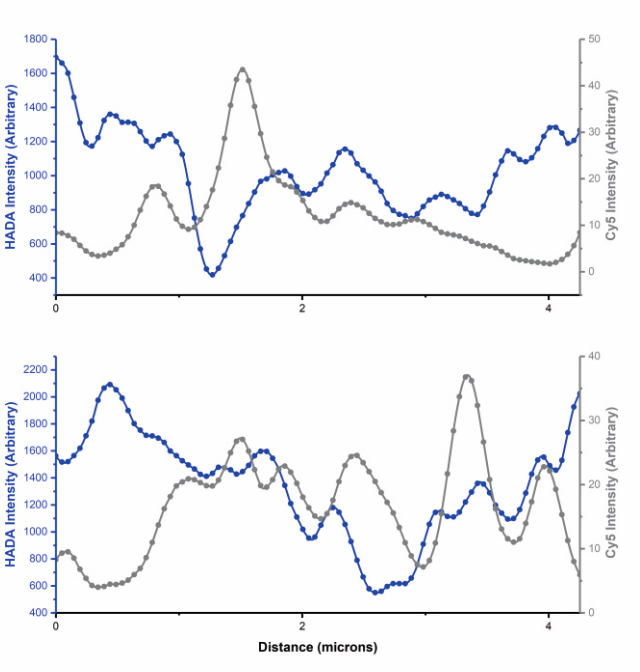

XiV

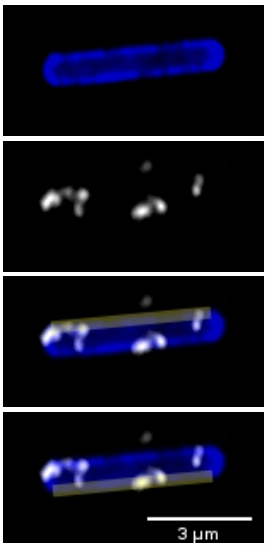

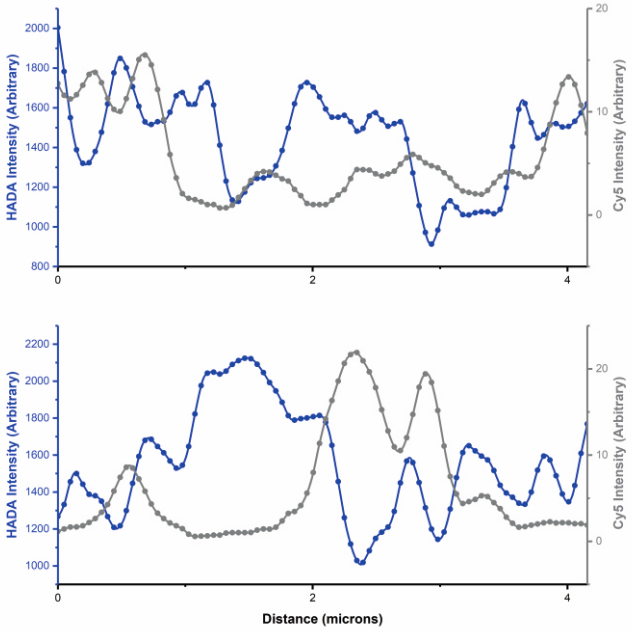

Supplementary Figure 2S3d

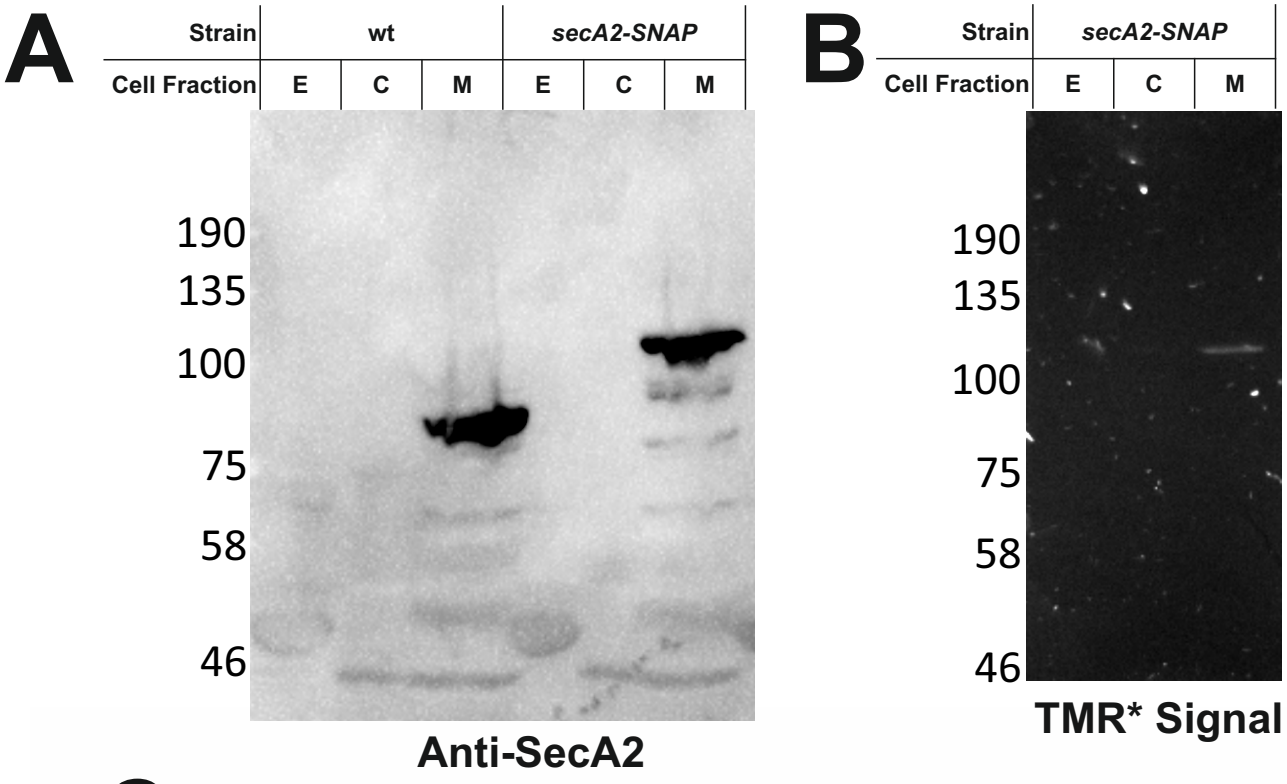

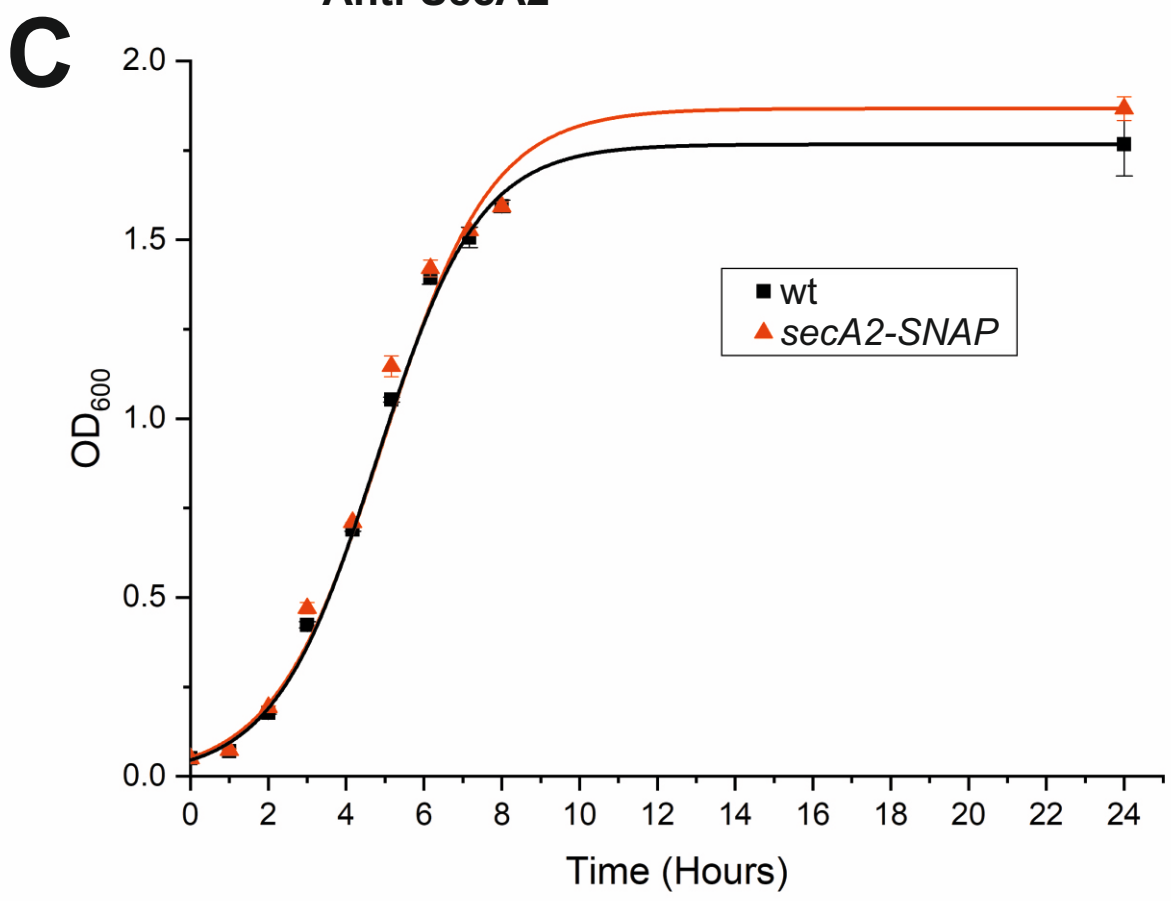

Supplementary Figure 4S1

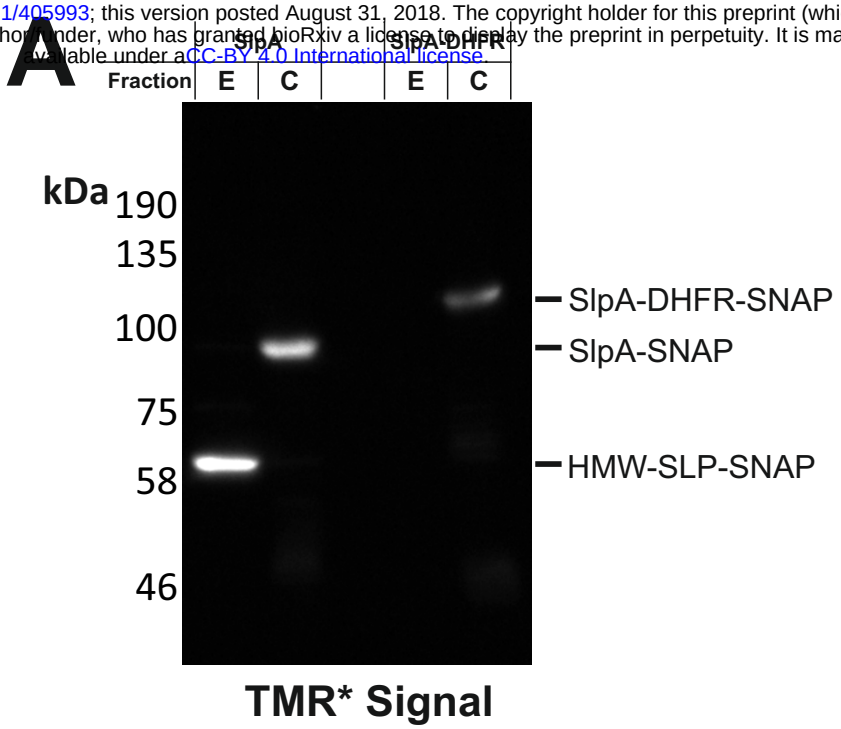

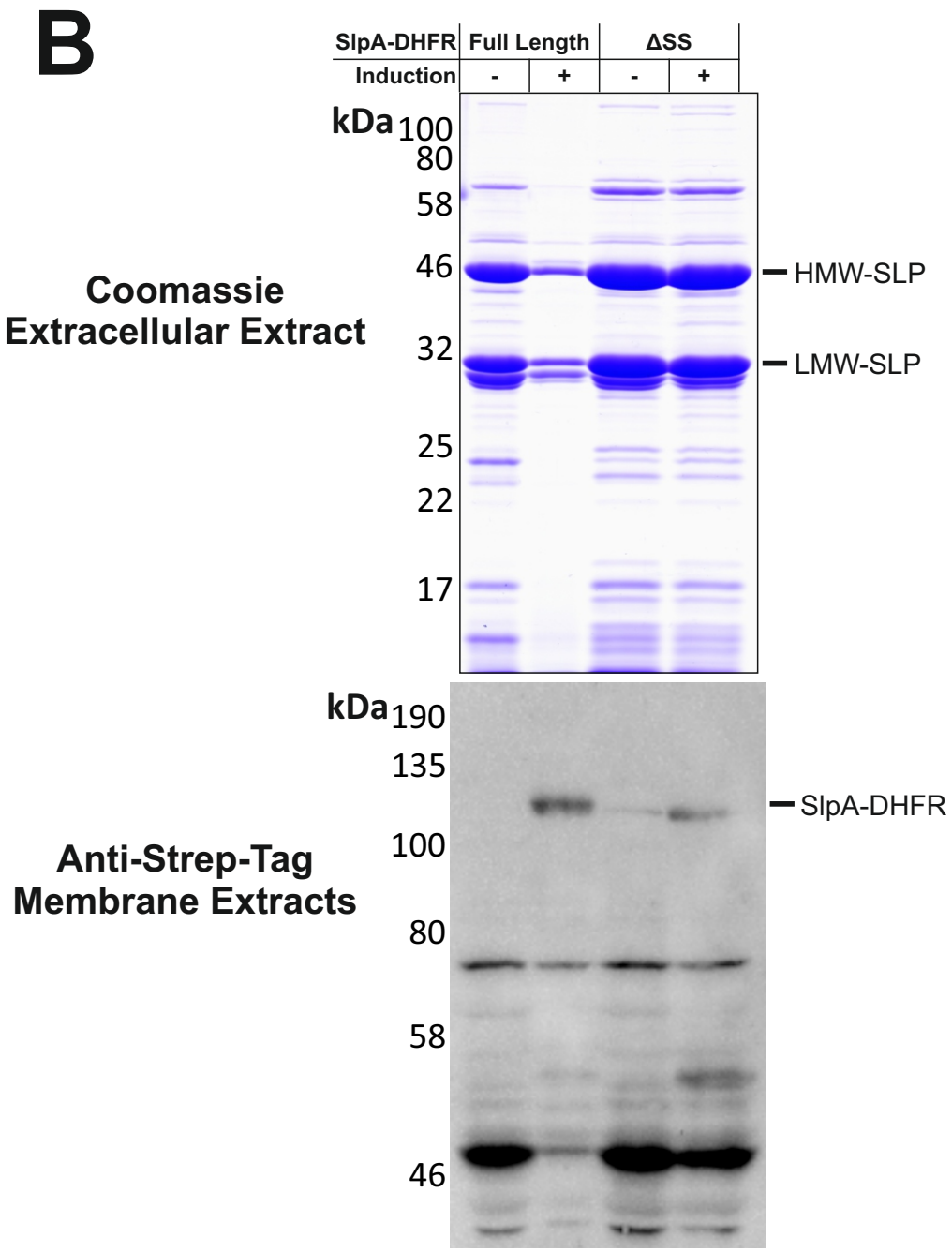

Supplementary Figure 5S1

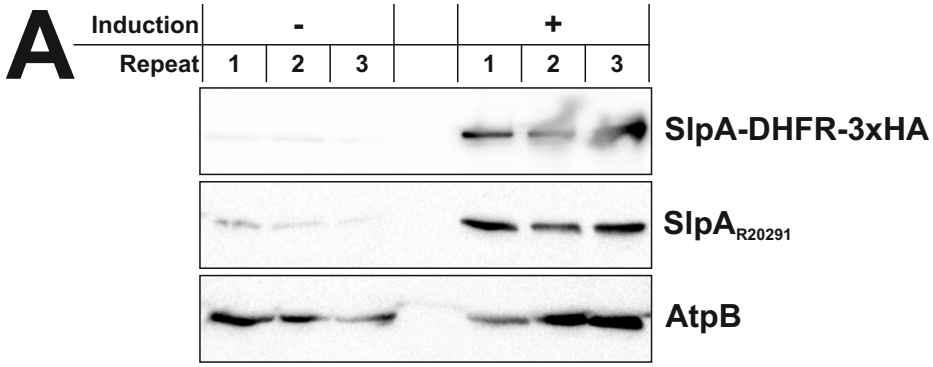

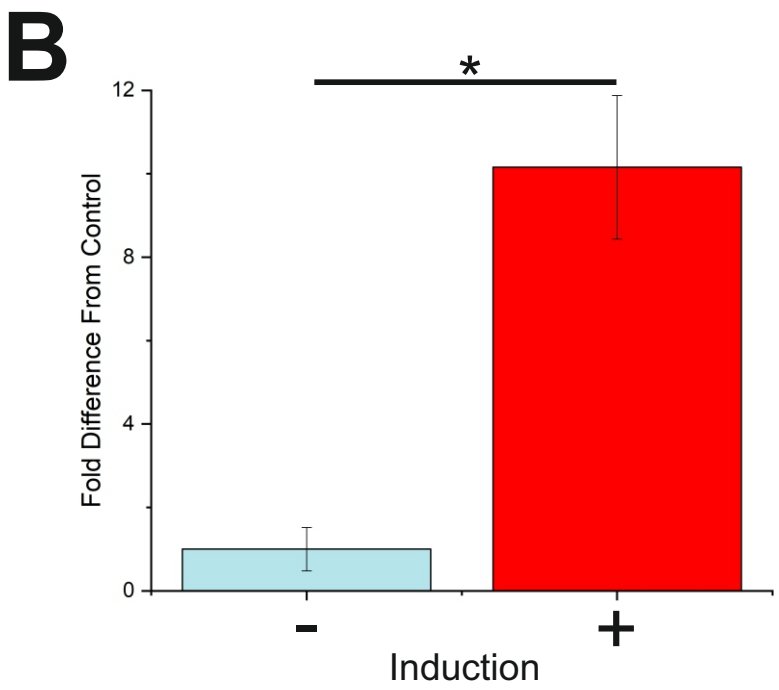

Supplementary Figure 5S2

Table 1: Strains, plasmids and oligonucleotides used in this study

Strain	Characteristics	Source
630	C. difficile strain 630	[1]
R20291	C. difficile strain R20291	[2]
CA434	E. coli strain CA434 (HB101 carrying R702)	[3]
CA434/SlpA$_{R20291}$	CA434 containing pRPF233 (P_{tet} SlpA$_{R20291}$)	[4]
CA434/SlpA$_{R20291::}$LMW Tc	CA434 containing pRPF238 (P_{tet} SlpA$_{R20291}$::LMW-Tc)	This Study
CA434/SlpA$_{630}$-DHFR-SNAP	CA434 containing pJAK085 (P_{tet} SlpA$_{630}$-hDHFR-Myc-SNAP)	This Study
CA434/SlpA$_{630}$-SNAP	CA434 containing pJAK023 (P_{tet} SlpA$_{630}$-SNAP)	This Study
CA434/SlpA$_{630}$-DHFR-Strep	CA434 containing pPOE002 (P_{tet} SlpA$_{630}$-hDHFR-Strep Tag II)	This Study
CA434/ΔSS-SlpA$_{630}$-DHFR-Strep	CA434 containing pPOE011 (P_{tet} Δsignal Sequence(ΔN2-A24)-SlpA$_{630}$-hDHFR-Myc-Strep TagII)	This Study
CA434/SlpA$_{630}$-DHFR-3xHA	CA434 containing pPOE003 (P_{tet} SlpA$_{630}$-hDHFR-Myc-3xHA)	This Study
CA434/SecA2::SecA2-SNAP	CA434 containing pPOE032 (pMTLSC7315 with secA2-Short Linker-SNAP)	This Study
630_secA2-SNAP	630 expressing genomic tagged SecA2-SNAP	This Study
630/SlpA$_{R20291}$	630 containing pRPF233 (P_{tet} SlpA$_{R20291}$)	This Study
630/SlpA$_{R20291::}$LMW Tc	630 containing pRPF238 (P_{tet} C. diff R20291 SlpA::Tc)	This Study
630/SlpA$_{630}$-DHFR-SNAP	630 containing pJAK085 (P_{tet} SlpA$_{630}$-hDHFR-Myc-SNAP)	This Study
630/SlpA$_{630}$-SNAP	630 containing pJAK023 (P_{tet} SlpA$_{630}$-SNAP)	This Study
630/SlpA$_{630}$-DHFR-Strep	630 containing pPOE002 (P_{tet} SlpA$_{630}$-hDHFR-Strep Tag II)	This Study
630/ΔSS-SlpA$_{630}$-DHFR-Strep	630 containing pPOE011 (P_{tet} Δsignal Sequence(ΔN2-A24)-SlpA$_{630}$-hDHFR-Myc-Strep TagII)	This Study

630/SlpA$_{630}$-DHFR-3xHA	630 containing pPOE003 (P_{tet} SlpA$_{630}$-hDHFR-Myc-3xHA)	This Study
630/SlpA$_{630}$-DHFR-3xHA	R20291 containing pPOE003 (P_{tet} C. diff 630 SlpA-hDHFR-Myc-3xHA)	This Study

Plasmid	**Characteristics**	**Source**
pRPF233	P_{tet} SlpA$_{R20291}$	[4]
pRPF238	P_{tet} SlpA$_{R20291}$::LMW-Tc	This Study
pJAK085	P_{tet} SlpA$_{630}$-hDHFR-Myc-SNAP	This Study
pPOE023	P_{tet} SlpA$_{630}$-SNAP	This Study
pPOE002	P_{tet} SlpA$_{630}$-hDHFR-Strep Tag II	This Study
pPOE011	P_{tet} Δsignal Sequence(ΔN2-A24)-SlpA$_{630}$-hDHFR-Myc-Strep TagII	This Study
pPOE003	P_{tet} SlpA$_{630}$-hDHFR-Myc-3xHA	This Study
pPOE032	pMTLSC7315 with secA2-Short Linker-SNAP	This Study
pJAK067	pMTLSC7315 with SecA2-SNAP	This Study
pMTLSC7315		[5]

Oligo	**Sequence**	**Function**	**Source**
RF721	GTCACTCGAGGTTCGTCCGCTGAATTGTATTGTTGC	XhoI-DHFR_Fwd	This Study
RF722	GTCACTCGAGCAGATCTTCTTCGCTAATC	DHFR_XhoI_Rev	This Study
RF723	GTCAGGATCCTCATCATTACAGATCTTCTTCGCTAATC	DHFR_Myc_BamHI_Rev	This Study
RF789	GCAACTACTGGAACACAAG	delete SlpA signal sequence For	This Study
RF790	CATTTCTTAAATTCCTCCCAAC	delete SlpA signal sequence Rev	This Study
RF811	CCGGACTATGCAGGATCCTATCCATATGACGTTCCAGATTACGCTCCGTAAGGATCCTATAAGTTTTAATAAAAC	Add triple HA tag on SlpA-DHFR For	This Study

RF812	GACGTCATAGGGATAGCCCGCATAGTCAGGAAC ATCGTATGGGTAAACCTCGAGCAGATCTTCTTC	Add triple HA tag on SlpA-DHFR Rev	This Study
RF1079	TGCTAAGGCCGATAAAGATTGTGAAATGAAGAG	Change linker in pJAK067 (SecA2-SNAP in pMTLsc7315) to AEAAAKA For	This Study
RF1080	GCTGCCTCAGCGTTAAATTTATATAAGTATTGCA CTG	Change linker in pJAK067 (SecA2-SNAP in pMTLsc7315) to AEAAAKA Rev	This Study
RF635	CGTAGAAATACGGTGTTTTTTGTTACCCTATCAA TCTATAAATTAAATGTTGTCC	SecA2 left with 315 overlap	This Study
RF638	GGGATTTTGGTCATGAGATTATCAAAAAGGCAT ATTACCTTTAACAGTTAATCTATATC	SecA2 right with 315 overlap	This Study

[1] M. Sebaihia, B.W. Wren, P. Mullany, N.F. Fairweather, N. Minton, R. Stabler, N.R. Thomson, A.P. Roberts, A.M. Cerdeno-Tarraga, H. Wang, M.T. Holden, A. Wright, C. Churcher, M.A. Quail, S. Baker, N. Bason, K. Brooks, T. Chillingworth, A. Cronin, P. Davis, L. Dowd, A. Fraser, T. Feltwell, Z. Hance, S. Holroyd, K. Jagels, S. Moule, K. Mungall, C. Price, E. Rabbinowitsch, S. Sharp, M. Simmonds, K. Stevens, L. Unwin, S. Whithead, B. Dupuy, G. Dougan, B. Barrell, J. Parkhill, The multidrug-resistant human pathogen Clostridium difficile has a highly mobile, mosaic genome, Nat Genet 38(7) (2006) 779-86.

[2] Great Britain. Commission for Healthcare Audit and Inspection., Investigation into outbreaks of Clostridium difficile at Stoke Mandeville Hospital, Buckinghamshire Hospitals NHS Trust, Commission for Healthcare Audit and Inspection, London, 2006.

[3] D. Purdy, T.A. O'Keeffe, M. Elmore, M. Herbert, A. McLeod, M. Bokori-Brown, A. Ostrowski, N.P. Minton, Conjugative transfer of clostridial shuttle vectors from Escherichia coli to Clostridium difficile through circumvention of the restriction barrier, Mol Microbiol 46(2) (2002) 439-52.

[4] J.A. Kirk, D. Gebhart, A.M. Buckley, S. Lok, D. Scholl, G.R. Douce, G.R. Govoni, R.P. Fagan, New class of precision antimicrobials redefines role of Clostridium difficile S-layer in virulence and viability, Sci Transl Med 9(406) (2017).

[5] S.T. Cartman, M.L. Kelly, D. Heeg, J.T. Heap, N.P. Minton, Precise manipulation of the Clostridium difficile chromosome reveals a lack of association between the tcdC genotype and toxin production, Appl Environ Microbiol 78(13) (2012) 4683-90.